Susceptibility to Neutralization by Broadly Neutralizing Antibodies Correlates with Infected Cell Binding for a Panel of Clade B HIV Reactivated from Latent Reservoirs

Yanqin Ren[*1,2], Maria Korom[*1], Ronald Truong[1], Dora Chan[1], Szu-Han Huang[1,2], Colin C. Kovacs[3], Erika Benko[3], Jeffrey T. Safrit[4], John Lee[4], Hermes Garbán[5], Richard Apps[1], Harris Goldstein[6], Rebecca M. Lynch[1#], R. Brad Jones[1,2#]

[1]Dept. of Microbiology Immunology and Tropical Medicine, The George Washington University, Washington, DC, 20037, USA.
[2]Infectious Disease Division, Weill Cornell Medical College, New York, New York, 10021, USA.
[3]Maple Leaf Medical Clinic, Toronto, ON M5G 1K2, Canada.
[4]NantBioScience INC. | NantKwest LLC., 9920 Jefferson Blvd, Culver City, CA 90232, USA.
[5]NantWorks, LLC., 9920 Jefferson Blvd, Culver City, CA 90232, USA.
[6]Dept. of Pediatrics and Microbiology & Immunology, Albert Einstein College of Medicine, New York, 10461, USA.

[*]These authors contributed equally
[#]These are co-senior authors

Correspondence and requests for materials should be addressed to
R. Brad Jones (email: rbjones@med.cornell.edu)
or Rebecca Lynch (email: rmlynch@email.gwu.edu).

Running title: bNAb binding and neutralization of HIV from reservoirs

Word count for the abstract: 223
Word count for the text: 7395

Abstract

Efforts to HIV cure are obstructed by reservoirs of latently infected $CD4^+$ T-cells that can re-establish viremia. Broadly neutralizing HIV-specific antibodies (bNAbs), defined by unusually high neutralization breadths against globally diverse viruses, may contribute to the elimination of these reservoirs by binding to reactivated cells, targeting them for immune clearance. However, the relationship between neutralization of reservoir isolates and binding to corresponding infected primary $CD4^+$ T-cells has not been determined. Thus, the extent to which neutralization breadths and potencies can be used to infer the corresponding parameters of infected-cell binding is currently unknown. We assessed the breadths and potencies of bNAbs against 36 viruses reactivated from peripheral blood $CD4^+$ T-cells of ARV-treated HIV-infected individuals, using paired neutralization and infected-cell binding assays. Single antibody breadths ranged from 0–64% for neutralization (IC_{80}≤10μg/ml) and 0–89% for binding, with two-antibody combinations reaching 0-83% and 50-100%, respectively. Infected-cell binding correlated with virus neutralization for 10 out of 14 antibodies (e.g. 3BNC117, r=0.87, p<0.0001). Heterogeneity was observed, however, with a lack of significant correlations for 2G12, CAP256.VRC26.25, 2F5, and 4E10. Our results provide guidance on the selection of bNAbs for interventional cure studies; both by providing a direct assessment of intra- and inter-individual variability in neutralization and infected cell binding in a novel cohort, and by defining the relationships between these parameters for a panel of bNAbs.

Importance

Although anti-retroviral therapies have improved the lives of people who are living with HIV, they do not cure infection. Efforts are being directed towards harnessing the immune system to eliminate the virus that persists, potentially resulting in virus-free remission without medication. HIV-specific antibodies hold promise for such therapies owing to their abilities to both prevent the infection of new cells (neutralization), and also to direct the killing of infected cells. We isolated 36 HIV strains from individuals whose virus was suppressed by medication, and tested 14 different antibodies for neutralization of these viruses and for binding to cells infected with the same viruses (critical for engaging natural killer cells). For both neutralization and infected-cell binding, we observed variation both between individuals, and amongst different viruses within an individual. For most antibodies, neutralization activity correlated with infected cell binding. These data provide guidance on the selection of antibodies for clinical trials.

Introduction

Modern antiretroviral (ARV) drug regimens effectively suppress HIV replication, but are unable to cure infection. Interruption of ARV therapy thus results in rapid viral rebound and disease progression. A critical aspect of HIV persistence in the context of ARV therapy is the establishment of latent infection in long-lived resting memory $CD4^+$ T-cells (1-3). Evidence from *in vitro* latency models supports that these reservoirs can be eliminated by combining latency reversal agents (LRAs), which induce the expression of viral antigens, with enhanced immune effectors; a paradigm referred to as “kick and kill” or, alternatively, as “shock and kill” (4-6). One strategy to harness immune effectors for these strategies is to target reactivated infected cells with HIV-specific antibodies, resulting in the engagement of natural killer (NK) cells, monocytes, and granulocytes which eliminate infected cells through antibody-dependent cell-mediated cytotoxicity (ADCC) and/or antibody-dependent cell-mediated phagocytosis (ADCP) (7-9). For this purpose, it will be crucial for the HIV-specific antibodies to bind to Env protein expressed on the surface of the reactivated latent infected cells. The current study focuses on correlating the susceptibility of neutralization against viral isolates reactivated from patient $CD4^+$ T-cells by a panel of HIV-specific broadly neutralizing antibodies (bNAbs) with their capacity to bind to Env expressed by the reactivated latent infected cells, thereby providing guidance on the selection of bNAbs to optimally support the clinical translation of kick and kill strategies.

The antigenic variability of the HIV Envelope protein poses a substantial challenge to the development of both vaccines and immunotherapeutics (10-12). The past 10 years have seen the identification of a growing number of 'broadly neutralizing antibodies' (bNAbs), defined as such based on their activity against globally diverse HIV isolates (13-22) [reviewed in (23-26)]. Recent clinical trials have established that passive infusion with bNAbs during chronic HIV infection can temporarily suppress virus replication in individuals whose virus does not escape (27-29), and modestly delay viral rebound during anti-retroviral treatment interruption (30, 31). Additionally, passive immunization with bNAbs has attracted interest as a means of supplying the immune effector component of kick and kill HIV eradication strategies (given that virus has typically escaped from autologous antibody responses). This has led to the initiation of additional preclinical trials, as well as pilot clinical studies aimed at testing the abilities of combinations of bNAbs and latency reversing agents (LRAs) to reduce or eliminate latent HIV reservoirs (e.g. ClinicalTrials.gov NCT03041012, NCT02850016).

Three primary factors argue for the prioritization of bNAbs, versus other types of HIV-specific antibodies, for clinical trials aimed at reducing latent reservoirs through a kick and kill mechanism. First, there is extensive clinical experience with, and safety data on, several bNAbs from their use in passive infusion trials; facilitating their advancement into combination studies with LRAs. Second, the ability to exert the dual activities of neutralizing free virus in addition

123 to mediating ADCC would be favorable for an antibody therapeutic. Third, the
124 antigenic diversity of HIV, both within a given individual's latent reservoir and at a
125 population level, poses a challenge to the development of curative therapeutics,
126 motivating the prioritization of Abs with broad reactivity. With respect to the latter
127 point, while it stands to reason that an Ab with broad neutralizing activity is likely
128 to exert a similar breadth of infected-cell binding, this cannot be assumed to be
129 the case. Infected cell binding is a prerequisite for, and correlates closely with,
130 ADCC activity (8, 32-34). The conformations of Env on free virions that must be
131 targeted to achieve neutralization may differ from those on infected cells that
132 must be bound to trigger ADCC. For example, binding of Env on an infected cell
133 to CD4 on that same cell (i.e: in *cis*) may both partially occlude the CD4 binding
134 site (CD4bs) and induce gp120 shedding, while exposing CD4-induced (CD4i)
135 epitopes and gp41 stumps (35); thus, antigenically changing the protein on a cell
136 as compared to the virion. Although CD4i antibodies commonly arise during
137 infection (36), and have the potential to mediate ADCC against liganded versions
138 of the Env protein, the addition of sCD4 mimetics has been necessary to
139 increase sensitivity of infected cells to ADCC by these antibodies (37, 38).
140 Furthermore, the possibility exists that viral diversity may differentially affect cell-
141 surface Env versus virion-associated functional Env trimers, potentially in
142 unexpected ways. Thus, broadly neutralizing antibodies present the possibility of
143 infusing multi-functional antibodies that target genetically diverse viruses on
144 epitopes that do not require CD4 binding for epitope exposure; however, broad
145 neutralizing activity may not equate to broad infected-cell binding. Of note, the

bNAbs tested in study all share the same IgG1 Fc domain, differing only in their Fab fragments. The current study thus focuses on providing guidance with respect to the selection of the antigen binding Fab fragments of Abs for use in cure strategies. To maximize potency, these Fab fragments may ultimately need to be combined with Fc domains that are designed to maximally engage ADCC effectors (39).

A limited number of studies have thus far assessed the breadths of infected-cell binding and/or ADCC activity by bNAbs in relation to neutralizing activity, and these have reported somewhat conflicting results. In testing 8 viral isolates reactivated from the latent reservoirs of ARV-treated individuals, Bruel *et al.* reported that a panel of bNAbs (including 3BNC117) could eliminate HIV infected cells by mediating ADCC (8), and that their breadth of virus recognition was higher than with non-neutralizing antibodies (32). In contrast, Mujib *et al*. reported a lack of infected-cell binding and ADCC activity by 3BNC117 against a multi-clade panel of HIV (40), suggesting a lack of correspondence with its breadth of neutralizing activity (15). Although this relationship has been explored indirectly, to our knowledge, only one study has directly compared infected cell binding or ADCC of bNAbs versus neutralizing activity across different viral isolates. This study showed a correlation between these functions, but was limited to the use of two viral isolates of HIV (NL4-3 and JR-FL) and SHIV AD8-EO (34). We therefore perceived a need to define the relationship between

168 neutralization and infected cell binding of clinically relevant bNAbs to HIV
169 produced by reactivated latent infected $CD4^+$ T cells.
170
171 In the current study we assessed, in parallel, virus neutralization and
172 infected primary $CD4^+$ T-cell binding of bNAbs against a panel of 36 viruses that
173 were reactivated from the latent reservoirs of 8 ARV-treated individuals by
174 quantitative viral outgrowth assays (QVOA) (41) (see schematic, **Fig 1**). We
175 defined the intra- and inter- patient breadths and potencies of both neutralization
176 and infected cell binding activity of these bNAbs against reactivated reservoir
177 viruses from a geographically localized population of clade B infected individuals.
178 For all bNAbs that demonstrated appreciable neutralizing activity, this correlated
179 closely with infected cell binding. This represents the most comprehensive study
180 to date using a large panel of bNAbs, which target a range of different epitopes
181 but share the same IgG1 Fc domain, against a panel of *ex vivo* reservoir
182 reactivated viruses to quantify both neutralization and binding to infected cells.
183
184 **Results**
185
186 **Virus Neutralization Profiles of bNAbs and bNAb Combinations Against**
187 **Reactivated Reservoir Viruses**
188
189 To test the ability of bNAbs to neutralize reservoir virus, we obtained a
190 panel of 14 bNAbs that are currently being developed for clinical use in humans

and categorized these by their targeted epitope (**See Methods**). We measured the neutralizing activities of these bNAbs against 36 viral isolates that had been reactivated from the latent reservoirs of 8 individuals from limiting dilution quantitative viral outgrowth assays (QVOA) (**Fig 1 and 2A**). The V3-glycan-specific bNAbs PGT121 and 10-1074 and the V1V2-specific bNAb PG9 exhibited potent but relatively narrow activity, exhibiting detectable neutralization (IC_{50} < 50 μg/ml) of 53 - 69% of viruses, with geometric mean IC_{50} values ranging from 0.3 – 0.6 μg/ml (**Fig 2B**). In contrast, the CD4 binding site (CD4bs)-specific antibodies VRC01, VRC07-523, N6 and 3BNC117, as well as the MPER-targeting antibody 10E8 exhibited broad activity, with a detectable neutralization 77 - 100% of viruses (IC_{50} < 50 μg/ml), but with substantially higher IC_{50} values (geometric mean IC_{50} between 2.1 – 8.9 μg/ml) (**Fig 2B**). These trends parallel previous reports using pseudovirus assays, which also observed that CD4bs antibodies and 10E8 were generally much broader but less potent than V3-glycan and V1V2 apex antibodies (42, 43). In the current experiment, CAP256.VRC26.25 only neutralized 9 of 36 reactivated reservoir viruses (26%) with a detectable IC_{50} (IC_{50} < 50 μg/ml) (**Fig 2B**). Because CAP256.VRC26.25 has been reported to preferentially neutralize subtype C, and the QVOA viral isolates tested here are all subtype B (**Table 1**), the low neutralization breadth we observed is compatible with published data (22). 4E10 and 2F5 are known to be less broad and potent than more recently published antibodies, so their lack of breadth against these viruses is expected. One exception to the general agreement between our data and those from published pseudovirus panels was

for 2G12 which, although not broadly neutralizing against genetically diverse viruses, has been shown to potently neutralizes subtype B viruses in published pseudovirus panels (19, 44), but we observed only weak neutralization in our assays, with only two viruses reaching 80% neutralization (**Fig 2**).

We frequently observed high degrees of similarity in neutralization sensitivities within an individual's viral quasispecies, consistent with genetic relatedness. For example, the five viral isolates from CIRC1096 were all sensitive to neutralization by CD4bs and MPER antibodies, but resistant to V3-glycan and V1V2 antibodies (**Fig 2B & C**). Exceptions to this, however, were not uncommon. For example, for the four QVOA viruses from OM5346, two of these viruses (#2 and #4) were highly sensitive to V1V2 antibodies (PG9, CAP256-VRC26.25, PGDM1400) and resistant to V3-glycan antibodies (PGT121, 10-1074 and 2G12) whereas virus #3 exhibited the opposite sensitivity profile (**Fig 2B & C**). Overall, of the 112 study participant / bNAb combinations (8 participants x 14 bNAbs) there were only 14 cases where a single bNAb provided coverage of each of the viral isolates tested from a given participant (IC_{80} ≤ 10 μg/ml, **Fig 2C in Cyan Bold**).

Given the limitations observed above in the breadths of coverage and potential escape of any single bNAb, it is likely that any clinical intervention would require combinations of multiple bNAbs to be effective. We therefore calculated the summed breadths of all combinations of two of the bNAbs tested in this

study. We determined breadth coverage by using an IC_{80} ≤ 10 μg/ml as the cut-off for the geometric mean sensitivity of the quasispecies, based on our previous demonstration that this concentration correlated with reduction in viremia in bNAb-treated clinical trial subjects (29). The combination of N6 with 10-1074 showed the greatest breadth of coverage, at 83% (IC_{80} ≤ 10 μg/ml) (**Fig. 2D**), followed by the combination of VRC07-523 and 10-1074, which displayed an IC_{80} ≤ 10 μg/ml for 81% of the reservoir virus isolates. Several antibody combinations displayed an IC_{80} ≤ 10 μg/ml for 78% of the reservoir virus isolates: N6 and PGT121, VRC07-523 and PGT121, 3BNC117 and 10-1074, 3BNC117 and PG9, 10E8v4-V5R-100cF and 10-1074. Thus, two antibody combinations are able to provide broad neutralization coverage of reactivated reservoir viruses at an IC_{80} ≤ 10 μg/ml for this geographically discrete clade B infected population.

Infected-Cell Binding Profiles of bNAbs and bNAb Combinations Against Reactivated Reservoir Viruses

We next measured the binding of bNAbs to the surface of primary $CD4^+$ T-cells infected with the same reservoir virus isolates that had been assessed for neutralization. Activated $CD4^+$ T cells from HIV-uninfected donors were infected with reactivated reservoir viruses and stained with unconjugated bNAbs, followed by Alexa Fluor 647 anti-human IgG secondary antibody. These samples were also stained with HIV Gag to identify infected cells. We used a Median Fluorescence Intensity (MFI) ratio to quantify specific bNAb binding activity to

infected cells [MFI ratio = (MFI of bNAb staining in HIV-Gag^{+} cells) / (MFI of bNAb staining in HIV-Gag^{-} cells)] (**Fig 3A**). Since we had already established the geometric mean IC_{80} neutralization values for each virus, we opted to test infected-cell binding at two concentrations for each antibody: i) 5 μg/ml - selected based on titration experiments (data not shown) ii) geometric mean IC_{80} neutralization concentrations for each antibody (values are indicated below the table in **Fig 2C**).

In order to establish breadth, we defined binding as a MFI ratio > 2. In general, with the exception of VRC01, CD4bs Abs exhibited superior breadths of infected-cell binding, covering 83 – 89% of reservoir isolates when tested at the neutralization IC_{80} concentrations (**Fig 3C & D**). The binding potencies of CD4bs were relatively modest, however, with most exhibiting MFI ratios of between 2 - 4 (**Fig 3B & C**). The V3-Glycan antibodies PGT121, 2G12, and 10-074 exhibited more limited breadths as compared to CD4bs antibodies, but showed substantially higher levels of specific binding to cells infected with susceptible viruses, with many MFI ratios exceeding 5. Sensitivity/resistance profiles were generally related for different viral isolates from the same individual, e.g. 10-1074 bound strongly to all isolates from 5/8 participants (**Fig 3B**), but exhibited a lack of binding to all viruses from CIRC0196 (at both concentrations). Intra-patient variability was observed, however, for example with 1 out of 5 viruses from OM5162 exhibiting high sensitivity to 10-1074 and the remaining 4 exhibiting resistance. With the exception of CAP256.VRC26.25 [which is predominately

283 clade C specific (22)], the V1/V2 bNAbs showed potent binding activity,
284 particularly in the case of PG9 which, at IC_{80} concentration, showed high levels of
285 specific binding to 16 of 36 reservoir viruses with an MFI ratio greater than 4 (**Fig**
286 **3C**). Infected cell binding of MPER-specific antibodies varied: 10E8v4-V5R-
287 100cF (a version of 10E8 optimized for increased solubility and potency(45)) at 5
288 μg/ml, bound to 30 of 36 isolates, with high-level binding observed for 13 of these
289 (MFI ratios > 4). However, 10E8 and 10E8v4-V5R-100cF also showed
290 substantial binding to uninfected bystanders (Gag^- population) (see **Fig 3A**, right
291 panel for representative staining). In contrast, the MPER-specific bNAbs 2F5 and
292 4E10 exhibited generally narrow and weak binding of reservoir viral isolates (**Fig**
293 **3B & C**). Of note, virus #1 from patient OM5162 showed a highly distinct bNAb
294 binding profile as compared to other isolates from the same individual: it was
295 bound strongly by antibodies VRC07-523, 3BNC117, N6, PGT121, 10-1074 and
296 PGDM1400, whereas other autologous viral isolates were bound weakly if at all
297 by these bNAbs. Similarly, viruses from OM5346 showed intra-individual diversity
298 in binding to V3-glycan-specific bNAbs too, as shown PGDM1400 and PG9
299 bound robustly to viruses #1 and #3 (MFI ratio > 6), while no binding was
300 observed for viruses #2 and #4 (**Fig 3B & C**). Our data indicate both intra- and
301 inter-individual variability in binding to cells infected with reservoir viral isolates,
302 highlighting the limitations of using any single antibody in a therapeutic.
303
304 Achieving broad coverage of viral reservoir isolates in a population is likely
305 to require combinations of at least two bNAbs. To assess this in the current

population, we calculated the binding coverage of all possible two antibody combinations using the binding data obtained with the neutralization IC_{80} antibody concentration (MFI ratio > 2) (**Fig 3D**). All CD4bs (excluding VRC01) antibodies, when combined with 2G12 or V1/V2 antibodies or MPER antibodies (except for 4E10), reached ≥ 92% coverage. Notably, the combinations of 2G12 with VRC07-523 or N6, or 10E8 or 10E8v4-V5R-100cF reached 100% coverage, however, as previously mentioned, 10E8v4-V5R-100cF showed a high level of bystander binding in our *in vitro* assays. 3BNC117 + 2G12 and VRC07-523 + PG9 reached 97% coverage, thus representing promising combinations for targeting reactivated clade B reservoir viruses (**Fig 3D**).

With respect to the effects of the different concentrations of antibodies tested on binding, 10E8v4-V5R-100cF exhibited generally more favorable binding profiles (MFI ratios) at 5 μg/ml, due to a reduction in the background binding that was observed at its IC_{80} concentration of 9.3 μg/ml. In contrast, 10-1074 showed a lack of background binding even at 5 μg/ml, and thus displayed favorable binding profiles at this higher concentration, compared to its IC_{80} concentration at 0.7μg/ml (**Fig 3B & D**).

Infected Cell Binding Correlates with Elimination by ADCC

Our primary interest in assessing infected-cell binding is to predict the ability of a bNAb to direct ADCC against these cells. Infected cell binding is a prerequisite

for ADCC, and multiple studies have indicated that, where antibody Fc domains are matched (as all bNAbs tested here share the same IgG1), levels of binding correlate with ADCC activity (8, 32-34). To confirm this relationship under our experimental conditions, we performed paired infected cell binding and ADCC assays using two reservoir isolates (OM5334#7 and OM5162#1) in combination with 9 bNAbs. Two types of NK cells were tested in parallel as effectors: i) haNK cells (NantKwest) – a derivative of the NK-92 cell line (46) that has been enhanced for ADCC by expressing high affinity (ha) huCD16 V158 FcγRIIIa receptor, as well as engineered to express IL-2 (47) ii) Freshly isolated NK cells from the peripheral blood of an HIV-uninfected donor. Binding assays were performed in parallel with ADCC assays using the same conditions - 10μg/ml over a total of 7 hours at 37°C. For both haNK cells and primary NK cells, we observed moderate levels of NK-cell mediated elimination of HIV-infected cells in the absence of bNAbs, likely due in part to HIV-mediated downregulation of HLA molecules "missing self" (Fig 3E, F) (48, 49). As expected, we observed additional elimination of infected cells with the addition of bNAbs, and significant direct correlations between total levels of elimination of HIV-infected cells (haNK, $r = 0.69$, $p < 0.001$; primary NK cells, $r = 0.65$, $p < 0.001$), as well as ADCC-specific elimination of infected cells (% killing in +bNAb conditions - % killing in –bNAb conditions) (haNK, $r = 0.73$, $p < 0.0001$; primary NK cells, $r = 0.65$, $p < 0.001$) (**Fig 3E, F)**. Thus, our results are consistent with previous studies in indicating that infected cell binding is moderately predictive of ADCC activity for bNAbs with matched Fc domains.

352 **bNAbs Exert Differential Binding to Populations of Early (Gag^+CD4^+) Versus**
353 **Late (Gag^+CD4^-) HIV-Infected Cells**
354
355 The infection of a cell by HIV results in the progressive, and almost
356 complete, loss of surface CD4 expression, through the concerted actions of Nef,
357 Vpu, and Env(50-53). Thus, in short-term *in vitro* infections of activated $CD4^+$ T-
358 cells, Gag^+CD4^- cells represent a later stage of infection than their Gag^+CD4^+
359 counterparts (which have not yet downregulated CD4). Env is expressed at
360 substantially higher levels in late- versus early- infected cells. Thus, variations in
361 overall levels of antibody binding to total Gag^+ cells between different viral
362 isolates, as observed in **Fig 3**, may reflect not only intrinsic differences in bNAb
363 sensitivity but also differences in infection kinetics (different ratios of early: late
364 infected cells and therefore different levels of protein expression). We therefore
365 sought to refine our analysis of levels of bNAb binding by controlling for stage of
366 infection.
367
368 We assessed whether differential binding of bNAbs to early (Gag^+CD4^+)
369 versus late (Gag^+CD4^-) infected cells was present in our assays. Upon gating on
370 viable HIV-infected cells (lymphocytes, live cells, $CD3^+$, HIV-Gag^+), we observed
371 that some bNAbs, such as 3BNC117, 10-1074, and PG9 showing preferential
372 binding to late infected cells ($CD4^-$) (**Fig 4A**), while others, such as 10E8v4-V5R-
373 100cF, showing similar, or slightly higher binding to early versus late populations
374 (**Fig 4A**). To test this systematically, we selected virus/bNAb combinations that

showed specific binding (Gag^+/ Gag^- bNAb MFI ratio > 2 when tested at neutralization IC_{80} concentrations) and compared levels of bNAb binding in the Gag^+CD4^+ versus Gag^+CD4^- populations. We calculated fold differences between these early and late infected populations = (Geometric Mean MFI ratio of Gag^+CD4^-) / (Geometric Mean MFI ratio of Gag^+CD4^+). We observed that all gp120-specific bNAbs exhibited higher levels of binding to late-infected populations than to matched early-infected populations (Fold differences: 1.7 – 3.9, **Fig 4B**). In contrast, each of the gp41-specific bNAbs exhibited similar or slightly higher levels of binding to early- versus late- infected populations (Fold differences: 0.90 – 0.97, **Fig 4B**). A mechanistic explanation for this discrepancy is beyond the scope of the current manuscript. However, we raise the possibility that it may be related to the in *cis* interactions that have been shown to occur on early infected cells between gp120 and CD4 on the same cell surface(54). Binding of CD4 to functional trimers can induce gp120 shedding from Env trimers, and enhance exposure of the gp41 membrane proximal external region to antibody binding (55). Our data are consistent with such conformational differences in Env favoring gp41-specific antibody binding to early-infected cells.

One implication of these results is that the binding data presented in **Fig 3** - which was generated based on total Gag^+ cells – over-represents binding to early-infected cells for gp120-specific antibodies, and under-represents binding to late-infected cells. Data calculated based only on the late-infected populations show a substantially intensified binding profile for most of the bNAbs used in this

study – most notably for the CD4bs bNAbs and PG9 (binding @ geographic mean IC_{80} concentration, **Supplementary Fig 1**). A second implication is that cellular infection dynamics may impact the ability to detect relationships between infected-cell binding and virus neutralization. For example, if virus 1 replicated with faster kinetics than virus 2, and thus had a greater proportion of $Gag^{+}CD4^{-}$ versus $Gag^{+}CD4^{+}$ cells, then this would skew bNAb binding profiles in a way that was not intrinsic to the Env itself. To account for this, we have assessed these relationships based on both total Gag^{+} cells and on only the $Gag^{+}CD4^{-}$ late infected populations (below).

Virus Neutralization Correlates with Infected-Cell Binding for most bNAbs

The breadths and potencies of neutralizing activity of bNAbs against diverse HIV isolates have been extensively studied (13-22). In contrast, relatively few studies have assessed breadths and potencies of infected-cell binding, which is an important pre-requisite for ADCC (8, 32-34). Efforts to harness bNAbs to direct ADCC against infected cells would therefore benefit from an understanding of the degree to which infected cell binding can be inferred from neutralizing activity against a given virus. Our paired binding and neutralization data sets allowed us to assess this using a number of analytic approaches in regards to both concentrations of bNAbs used for binding assays and to stage of infection of target cells. With respect to bNAb concentrations, binding to infected cells was assessed for each bNAb at 5 μg/ml, and at the geometric mean IC_{80}

neutralization concentration of that antibody against the same panel of reservoir viruses. For the latter, this meant that some antibodies were tested at > 5 μg/ml (ex. 4E10 at 49.2 μg/ml), while other antibodies were tested at substantially lower concentrations (e.g. PGT121 at 0.6 μg/ml) (Geo Mean IC_{80} concentrations are given below the heat-map in **Fig 2C**). This approach thus seeks to normalize for intrinsic differences in avidity between different bNAbs. With respect to stage of infection of target cells, we separately tested for correlations between neutralization IC_{80} and binding to either total infected cells (Gag^{+}) or to late-infected cells ($Gag^{+}CD4^{-}$), based on the differential binding patterns described above. Of these, the most appropriate method for assessing the relationship between binding and neutralization likely depends on the question being asked. Importantly, however, the relationships that we observed, as described below, turned out to be conserved across these different approaches.

We first tested for correlations between neutralization IC_{80} and the level of binding (MFI ratio) at 5 μg/ml bNAb concentrations. As is described above, since cells in early versus late stages of HIV infection exhibit differential bNAb binding profiles, replication dynamics have the potential to impact overall assessments of binding. In order to increase our ability to discern Env-intrinsic relationships between binding and neutralization we therefore limited this initial analysis to the late-infected ($Gag^{+}CD4^{-}$) population. When all antibodies were considered together, we observed a significant, direct correlation between virus neutralization and infected cell binding ($p < 0.0001$, Spearman's $r = 0.63$) (**Fig**

444 **5A**). For each of the bNAbs that showed appreciable neutralizing activity
445 (VRC01, VRC07, 3BNC117, N6, PGT121, 10-1074, PGDM1400, PG9, 10E8,
446 and 10E8v4-V5R-100cF) we observed significant direct correlations between
447 neutralizing activity and infected-cell binding (**Fig 5B)**. The antibodies 2F5 and
448 CAP256.VRC26.25 showed little in the way of either neutralization or binding,
449 precluding the possibility of detecting a relationship between these factors. 2G12
450 and, to lesser extent, 4E10 were notable outliers as they showed appreciable
451 binding capacity to many of the viruses in this panel, but very little corresponding
452 neutralizing activity. This lack of potent neutralization activity is inconsistent with
453 data from pseudovirus assays, but in agreement with previous data using virus
454 produced from T-cells, suggesting that 2G12 sensitivity is particularly tied to the
455 source of virus (56-58).
456
457 Correlations between neutralization IC_{80} and binding as measured by
458 other approaches are presented as follows: i) binding of antibodies tested at 5
459 µg/ml concentrations to total infected population (all Gag^+) – **Supplementary Fig**
460 **2;** ii) binding of antibodies tested at IC_{80} neutralization concentrations to late
461 infected population (Gag^+CD4^-) – **Supplementary Fig 3;** iii) binding of antibodies
462 tested at IC_{80} neutralization concentrations to total infected population (all Gag^+)
463 – **Supplementary Fig 4**. Correlation coefficients varied across these different
464 analyses, with different approaches yielding stronger correlations for different
465 bNAbs, e.g. for 3BNC117: Spearman's r = 0.82 for 5 µg/ml total Gag^+
466 (**Supplementary Fig 2**) vs Spearman's r = 0.60 for IC_{80} concentration total Gag^+

(**Supplementary Fig 4**); for PGT121: Spearman's r = 0.47 for 5 μg/ml total Gag^+ (**Supplementary Fig 2**) vs Spearman's r = 0.71 for IC_{80} concentration total Gag^+(**Supplementary Fig 4**). Overall, however, each of the antibodies that exhibited a significant correlation by one analytic approach also exhibited significant correlations by the other three approaches, and vice versa for those lacking significant correlations. Thus, for 10 out of 14 bNAbs tested in this study, the ability of a bNAb to neutralize a given virus is strongly correlated with its ability to bind to a corresponding infected cell. In these *in vitro* assays, this correlation was robust enough to be observed with or without controlling for avidity of a given bNAb or for infection dynamics.

Discussion

The primary conclusion of the current study is that the ability of a given bNAb to neutralize clinical viral isolates is a strong correlate of its ability to bind to cell-surface Env on primary $CD4^+$ T-cells infected with the same virus. Furthermore, in comparing across a large panel of bNAbs, relative levels of infected-cell binding and virus neutralization continued to correlate – for example, 10-1074 showed both high-level infected-cell binding and potent neutralization compared to VRC01. Thus, we conclude that – with respect to the Fab component of Abs, when sharing the same Fc – the selection of Abs based on broad and potent neutralizing activity is very likely to also select for those that are suitable for infected-cell clearance. Of note, the reciprocal was not always true;

with 2G12 exhibiting reasonably potent and broad infected-cell binding, contrasted by a general lack of neutralization of these reservoir-derived primary isolate viruses. Though less strikingly, the MPER-specific bNAbs 2F5 and 4E10 also exhibited appreciable infected-cell binding (similar in breadths and magnitudes to VRC01), but with minimal neutralizing activity. We propose that the differences based on the directionality of this relationship may be related to the differential antigen conformational requirements for these two functions. For a bNAb to neutralize virus, it must bind functional Env trimers present on the surface of cells producing infectious virus. In contrast, an antibody that also binds to nonfunctional envelope proteins, such as gp41 stumps (59), may bind to infected cells to a greater degree than they mediate neutralization (if they neutralize at all). Thus, virus neutralization is a predictor of infected-cell binding, but the reciprocal relationship does not hold.

While it may be intuitive that virus neutralization would correlate with infected-cell binding, we do not feel that this could have been assumed to be the case without experimental evidence. The conformation of Envs may be affected by differences between the cell-surface vs virion environments, and this variability could impact different viral isolates. For example, in *cis* interactions between CD4 and Env on the surfaces of infected cells have been shown to induce gp120 shedding, and expose gp41 stumps. This has been reported to enhance infected-cell binding by gp41-specific Abs, while diminishing binding by gp120-specific Abs (35). Such an effect might differentially impact different

513 viruses – for example, Horwitz *et al*. reported that the R456K mutation on YU2
514 gp120 decreased gp120 shedding, which led to less bystander ($Gag^{-}CD4^{+}$)
515 binding (60). Our data are consistent with these observations, and provide further
516 evidence of *cis* binding of CD4 modulating the binding of bNAbs to infected-cells.
517 We find gp120-specific bNAbs bind preferentially to cells in a late stage of
518 infection ($CD4^{low}$) while gp41-specific bNAbs bind similarly or slightly better to
519 cells in an early stage of infection ($CD4^{high}$). To address more mechanisms of
520 these findings, future studies may benefit from including gp120/gp41 interface
521 bNAbs, such as 8ANC195 (61), PGT151, PGT158 (62). However, despite any
522 such differences between the virion and cell-surface environments, the ability to
523 neutralize virus was significantly correlated with infected-cell binding, and these
524 relationships held whether we considered all infected cells (Gag^{+}) or only late
525 infected cells ($Gag^{+}CD4^{-}$).
526
527 To investigate factors that may predict the efficacy of bNAb treatment to
528 contribute to HIV cure we felt it important to study the properties of bNAbs
529 against viruses derived from reactivated latent reservoirs. By combining a QVOA
530 approach with isolation of virus from dilutions of $CD4^{+}$ T cells from different ART-
531 suppressed patients where <50% of wells were $p24^{+}$, we were able to isolate
532 viruses that were likely clonal to test bNAb binding and neutralization profiles
533 (**Fig 1**) and assess both intra- and inter-patient variability. We observed a
534 considerable level of heterogeneity, even within a given individual, such that in
535 the majority of cases any single bNAb failed to provide universal coverage of an

individual's reservoir isolates. However, combinations of two antibodies provided broad coverage both within and across individuals, reaching up to 100% coverage as assessed by binding. Note that as our study population was derived from a single site (Toronto, Canada), from a clinical perspective this assessment of breadth is representative of what might be expected in a single-site study in a North American clade B infected cohort. We propose that the method presented here could be applied to different populations as a means of prioritizing antibody combinations for a given regional population of patients and personalizing individual HIV cure strategies as ART drug resistance is used to guide ART therapy. Clinical use of the QVOA assay will likely be limited by its expense, cell number requirements, and protracted timeline (14 days) for results. However, a notable opportunity is present in the fact that infectious clonal autologous reservoir viruses are generated as a byproduct of the primary measurement. The pairing of quantitative and qualitative assessments of the HIV reservoir in this way has been previously termed the Q^2VOA (63).

The potencies of neutralization observed in the current study are overall weaker than those that have been previously reported using pseudovirus assays – most notably for 2G12, which failed to achieve 80% neutralization for all but two viruses. While this is likely due in part to our use of clinical viral isolates, which are generally less sensitive to bNAbs than laboratory-adapted viruses (64, 65), we also note the role of virus producing cells in modulating sensitivity to neutralization. Studies addressing this issue have reported that T-cell derived

559 virus is more resistant to neutralization than pseudovirus generated by
560 transfected 293T cells and, in particular, that replication competent virus
561 produced by PBMCs are more neutralization resistant than Env matched
562 pseudoviruses (56-58). However, there appear to be antibody-specific
563 differences in the level of influence that a producer cell has on sensitivity to
564 neutralization. For example, one study reported that PG9 is not very sensitive to
565 differences in producer cell (66), while large differences in IC_{50} have been
566 reported between T cell and pseudovirus for antibody 2G12 (56, 57). These data
567 suggest that producer cells differentially influence the conformations of Env on
568 resulting virions, as well as their densities and glycosylation, or numbers of
569 gp120 molecules in the viral membrane. As PG9 preferentially targets well-
570 ordered, closed, trimeric viral spikes, it indicates that an equal number of well-
571 folded spikes exists on virions produced by either cell type, whereas perhaps
572 bNAbs such as 2G12 can bind equally well to mis-folded trimers and are
573 therefore more sensitive to increases in the latter. Furthermore, the epitopes of
574 certain antibodies, such as 2G12, include glycans, and producer cells can affect
575 glycosylation patterns of gp120 (66). Thus, in addition to the comparison
576 between neutralization and infected-cell binding, the current study contributes a
577 reassessment of bNAb neutralization potency that may be more clinically
578 applicable than data from pseudovirus assays.
579
580 In conclusion, our study provides novel insights into the relationship
581 between infected-cell binding and virus neutralization that may help to guide

582 immunotherapeutic strategies aimed at either curing infection, or enabling
583 durable immune control of viral replication. The degree of intra- and inter-
584 individual variation in bNAb sensitivity within even this geographically discrete
585 clade B population reinforces the importance of utilizing combinations of at least
586 two bNAbs in such therapies. Screening reactivated reservoir viruses for
587 sensitivity to bNAbs, either at an individual or population level, can help select
588 antibody combinations for optimal coverage – for example, with combinations of
589 PG9 and either 3BNC117 or N6 providing potent infected-cell binding coverage
590 of 94% and 72-78% coverage of neutralization (IC_{80} ≤ 10μg/ml) of viruses in the
591 current study population. For the bNAbs that exhibited correlations between
592 infected-cell binding and neutralization, our study indicates that screening for
593 either one of these factors is sufficient to infer that both functions will be present
594 against reactivated reservoir viruses. Consistent with previous studies, we also
595 confirmed that this infected cell binding – as measured by our assay – correlated
596 well with NK cell mediated ADCC, suggesting that it is a reasonable surrogate. It
597 will be of interest, however, for future studies to build upon these results with
598 more extensive functional assays (potentially using varying Fc domains and/or
599 effector cells). Such future directions could potentially uncover more subtle
600 aspects of the relationship between virus neutralization and the targeting of cell-
601 mediated Fc-dependent functional activities against infected cells, which may
602 lead to the elimination of latent reservoirs.
603
604

Materials and Methods

Ethics Statement

All participants (HIV-infected individuals) were recruited from the Maple Leaf Medical Clinic in Toronto, Canada, through a protocol approved by the University of Toronto Institutional Review Board. Secondary use of the samples from Toronto was approved through the George Washington University Institutional Review Boards. All subjects were adults, and gave written informed consent. Clinical data for these participants are given in **Table 1**.

Broadly Neutralizing Antibodies

We used a panel of broadly neutralizing antibodies to HIV (bNAbs): CD4 binding sites antibodies (CD4bs)- VRC01, VRC07-523, 3BNC117, N6; V3-Glycan antibodies- PGT121, 2G12, 10-1074; V1/V2 antibodies- PGDM1400, CAP256.VRC26.25, PG9; MPER antibodies- 10E8, 10E8v4-V5R-100cF, 2F5, 4E10; and a positive control antibody HIV-IG and a negative control antibody 4G2-Hu for neutralization assays. Antibodies 10-1074, 2G12, and control antibody HIV-IG were obtained through the AIDS Reagent Program, Division of AIDS, NIAID, NIH from Dr. Michel C. Nussenzweig, Polymun Scientific and NABI and NHLBI, respectively. Dr. John Mascola provided antibody proteins 2F5 and 4E10, as well as all other antibody heavy- and light-chain expression plasmids. Antibody plasmids were expressed as full-length IgG1s from transient

transfection of 293F cells and purified by affinity chromatography using HiTrap Protein A HP Columns (GE Healthcare).

Quantitative viral outgrowth assay (QVOA)

Human CD4 T cells were enriched from the peripheral blood mononuclear cells (PBMCs) (Stemcell Technologies), processed from leukapheresis, which were drawn from long-term ARV-treated HIV-infected participants (**Table 1**). Cells were diluted into a serial concentration (2 million, 1 million, 0.5 million, 0.2 million and 0.1 million per well), and plated out into 24 well-plates and each concentration would have 12 wells. PHA and irradiated PBMCs were added to reactivate the infected cells and MOLT-4 cells were added 24 hours later to amplify the viruses. Media were changed every 3-4 days and p24 ELISA were run on day 14 to measure the amount of virus production.

p24 Enzyme-Linked Immunosorbent Assay

p24 enzyme-linked immunosorbent assay (ELISA) was performed with kit components obtained from National Cancer Institute, NIH. In brief, 96-well high binding microplates (Greiner Bio-One) were coated with capture antibody for overnight, and followed by 1% BSA solution blocking for overnight. Supernatants from QVOA wells were collected and lysed with 1% x-Triton buffer for 2 hours, followed by transferring to ELISA plates and incubating for 1 hour, 37^{o}C. Plates were then washed with PBST buffer (PBS+0.1% Tween-20) for 6 times and incubated with primary antibody for 1 hour, 37^{o}C. After 6 additional washes,

peroxidase labeled Goat anti-rabbit IgG secondary antibody (KPL) was added and incubated for another 1 hour at 37°C. After 6 additional washes, TMB substrate (Thermo Fisher) was added and developed for 15 mins, then stopped with stop solution (Biolegend). Absorbance was measured with SpectraMax i3x Multi-Mode microplate reader (Molecular Device) at OD450nm and 570nm. Cut offs for positive wells were set as > 2x the average of negative control values.

Neutralization assay

Neutralization of QVOA virus samples by bNAbs were measured using infection of Tzm-bl cells as described previously(30, 67). p24 protein in each virus sample was quantified by using the AlphaLISA HIV p24 Biotin-Free detection kit (Perkin Elmer, Waltham, MA), and input virus was normalized to 5-10ng/ml for the assay. 10µl of five-fold serially diluted mAbs from a starting concentration of 50µg/ml were incubated with 40µl of replication competent virus samples in duplicate for 30 minutes at 37°C in 96-well clear flat-bottom black culture plates (Greiner Bio-One). Tzm-bl cells were added at a concentration of 10,000 cells per 20µl to each well in DMEM containing 75µg/ml DEAE-dextran and 1µM Indinavir. Cell only and virus only controls were included on each plate. Plates were incubated for 24 hours at 37°C in a 5% CO_2 incubator, after which the volume of culture medium was adjusted to 200µl by adding complete DMEM containing Indinavir. 48 hours post-infection, 100µl was removed from each well and 100µl of SpectraMax Glo Steady-Luc reporter assay (Molecular Devices, LLC., CA)

673 reagent was added to the cells. After a 10-min incubation at room temperature to
674 allow cell lysis, the luminescence intensity was measured using a SpectraMax
675 i3x multi-mode detection platform per the manufacturers' instructions.
676 Neutralization curves were calculated comparing luciferase units to virus-only
677 control after background subtraction and fit by nonlinear regression using the
678 assymetric five-parameter logistic equation in GraphPad Prism (**Fig 2A**). The
679 50% and 80% inhibitory concentrations (IC_{50} and IC_{80}, respectively) were defined
680 as the antibody dilution that caused a 50% and 80% reduction in neutralization.
681
682 **bNAb binding assay**
683 All binding assays were tested with the unconjugated bNAbs. $CD4^+$ T cells
684 (which were all $CD3^+$) were isolated with the Human CD4 T cell enrichment kit
685 (Stemcell Technologies) and activated with CD3/28 antibodies (Biolegend) for 48
686 hours. Supernatants collected from QVOA wells ($p24^+$, the same viruses with
687 neutralization assay) were used for infection by adding into the activated $CD4^+$ T
688 cells, followed by spinnoculation for 1 hour and 6 days in culture with media
689 change every 3 days. Infection rate was checked on days 3 and 5 post infection.
690 When most of the infection reached >5%, bNAb staining were performed. Cells
691 were collected and washed twice with 2% FBS PBS, and then aliquoted into 96-
692 well plates (1 million cells per well). Unconjugated bNAbs were added according
693 to the outlined wells by diluting to a final concentration of 5μg/ml or neutralization
694 IC_{80} concentration, which was the Geo Mean of neutralized virus that generated
695 from neutralizing assay, and then incubated at 37ºC for 1 hour. Without washing,

696 the Alexa Fluor 647 labeled secondary antibody (Southern Biotech) was added
697 and incubated at 4°C for 30 minutes. After washing once with 2% FBS PBS,
698 surface antibodies mixture was added: BV786 anti-human CD3 (SK7, BD
699 Biosciences), Pacific Blue anti-human CD4 (RPA-T4, BD Pharmingen) and
700 LIVE/DEAD aqua (Life technology). 30 minutes later, cells were washed twice
701 and fixed/permeabilized with Fixation/Permeabilization Solution (BD Bioscience).
702 Anti-HIV-1 core antigen antibody (KC57-RD1, Beckman Coulter) was used to
703 stain intracellular HIV-1 gag protein. After two washes with 1x Perm/Wash buffer,
704 cells were detected by flow cytometry (BD Fortessa X-20), and data analysis was
705 performed with flowjo v10 (Treestar).
706
707 **Antibody mediated NK cell killing (ADCC) assay**
708 ADCC assays were performed with unconjugated bNAbs and one of two types of
709 NK cells: haNK cells (NantKwest), a NK-92 cell line which has been engineered
710 to express the high affinity (ha) CD16 V158 FcγRIIIa receptor, as well as
711 engineered to express IL-2 (47); and primary NK cells enriched from the PBMCs
712 of an HIV-negative donor (buffy coat from Gulf Coast Regional Blood Center)
713 using the Human NK cell enrichment kit (Stemcell Technologies). To generate
714 target cells, primary $CD4^+$ T-cells were enriched from the PBMCs of allogeneic
715 healthy donors and infected with reservoir viruses as for binding assays (see
716 above). Infections were monitored by flow cytometry, and ADCC assays were
717 performed when target cells were >5 % infected. Both types of NK cells were
718 treated with 10nM IL-15 superagonist complex, ALT-803 (68, 69) for 1 hour to

719 prime and activate them. Infected cells were collected and washed twice with 2%
720 FBS PBS. 2×10^5 cells/well were added into U-bottom 96-well plates.
721 Unconjugated bNAbs (VRC01, VRC07-523, 3BNC117, N6, PGT121, 2G12, 10-
722 1074, PGDM1400, PG9, A32 or no Ab) were added to final concentrations of
723 10μg/ml, and then incubated at 37°C for 2 hours. After this incubation, 4×10^5
724 ALT-803 treated NK cells were added to each well to give E:T ratios of 2:1.
725 bNAbs binding assays was performed in parallel with the ADCC assay with same
726 conditions but no NK cells added. Plates were centrifuged at 100×g for 30
727 seconds to bring target and effector cells into contact with each other, and then
728 incubated at 37°C, 5% CO_2. Cells were mixed by pipetting after 2 hours of
729 incubation, and then cocultured for an additional 5 hours. After a total of 7 hours
730 of co-culture, cells were washed twice with 2% FBS PBS, and stained with
731 fluorochrome-conjugated antibodies against: human IgG, CD3, CD56, CD4 (all
732 from Biolegend), as well as with a live/dead aqua amine reactive dye (Molecular
733 Probes). Cells were then fixed and permeabilized using the BD cytofix/cytoperm
734 kit and following the manufacturer's instructions. Intracellular HIV-Gag was then
735 stained with PE-conjugated anti-HIV-Gag (clone KC57, Beckman Coulter). Cells
736 were analyzed by flow cytometry (BD Fortessa X-20), and data analysis was
737 performed using flowjo v10 (Treestar). Frequencies of viable Gag^+ cells amongst
738 the $CD3^+$ cells (all targets) were determined. Killing (%) values were calculated
739 using the following formula: [% Gag^+ (of viable $CD3^+$ cells) in no NK cell no Ab
740 condition - % Gag^+ (of viable $CD3^+$ cells) in test condition] / [% Gag^+ (of viable
741 $CD3^+$ cells) cells in no NK cell no Ab condition] * 100%. ADCC (%) values were

742 calculated using the following formula: [% Gag^+ (of viable $CD3^+$ cells) in +NK
743 cells but no Ab condition - % of Gag^+ (of viable $CD3^+$ cells in test condition) / (%
744 of Gag^+CD3^+ cells +NK but no Ab condition) * 100%. Negative values were set
745 equal to zero.
746
747 **Statistical analysis**
748 Statistical analyses were performed using Prism 7 (GraphPad). Flow data were
749 analized with flowjo v10. The heat-maps were generated with Excel. Comparison
750 between MFI ratio of Gag^+CD4^+ and that of Gag^+CD4^- was using Wilcoxon
751 matched-pairs signed rank test. All correlations were calculated using using
752 Spearman's Rank-Order test.
753
754
755 **Acknowledgments**
756 We thank all of the study participants who devoted time to our research. We also
757 thank Kiera Clayton for helpful comments on the manuscript. Research reported
758 in this publication was supported by the National Institute of Allergy and
759 Infectious Diseases of the National Institutes of Health under award number
760 UM1AI126617 – the Martin Delaney 'BELIEVE' Collaboratory, with co-funding
761 support from the National Institute on Drug Abuse, the National Institute of
762 Mental Health, and the National Institute of Neurological Disorders and Stroke.
763 This work was also supported under NIH award numbers AI22391, AI31798,
764 MH12224, and by the NIH funded Center for AIDS Research grant P30 AI117970

765 which is supported by the following NIH Co-Funding and Participating Institutes
766 and Centers: NIAID, NCI, NICHD, NHLBI, NIDA, NIMH, NIA, FIC, and OAR. The
767 content is solely the responsibility of the authors and does not necessarily
768 represent the official views of the National Institutes of Health. The following
769 materials were supplied by the NIH AIDS Research and Reference Reagent
770 Program: broadly neutralizing antibodies, IL-2, MOLT-4 CCR5 cells.

771

References

1. Wong JK, Hezareh M, Gunthard HF, Havlir DV, Ignacio CC, Spina CA, Richman DD. 1997. Recovery of replication-competent HIV despite prolonged suppression of plasma viremia. Science 278:1291-5.
2. Finzi D, Hermankova M, Pierson T, Carruth LM, Buck C, Chaisson RE, Quinn TC, Chadwick K, Margolick J, Brookmeyer R, Gallant J, Markowitz M, Ho DD, Richman DD, Siliciano RF. 1997. Identification of a reservoir for HIV-1 in patients on highly active antiretroviral therapy. Science 278:1295-300.
3. Chun TW, Stuyver L, Mizell SB, Ehler LA, Mican JA, Baseler M, Lloyd AL, Nowak MA, Fauci AS. 1997. Presence of an inducible HIV-1 latent reservoir during highly active antiretroviral therapy. Proc Natl Acad Sci U S A 94:13193-7.
4. Shan L, Deng K, Shroff NS, Durand CM, Rabi SA, Yang HC, Zhang H, Margolick JB, Blankson JN, Siliciano RF. 2012. Stimulation of HIV-1-specific cytolytic T lymphocytes facilitates elimination of latent viral reservoir after virus reactivation. Immunity 36:491-501.
5. Deeks SG. 2012. HIV: Shock and kill. Nature 487:439-40.
6. Archin NM, Margolis DM. 2014. Emerging strategies to deplete the HIV reservoir. Curr Opin Infect Dis 27:29-35.
7. Kramski M, Parsons MS, Stratov I, Kent SJ. 2013. HIV-specific antibody immunity mediated through NK cells and monocytes. Curr HIV Res 11:388-406.
8. Bruel T, Guivel-Benhassine F, Amraoui S, Malbec M, Richard L, Bourdic K, Donahue DA, Lorin V, Casartelli N, Noel N, Lambotte O, Mouquet H, Schwartz O. 2016. Elimination of HIV-1-infected cells by broadly neutralizing antibodies. Nat Commun 7:10844.
9. Ferrari G, Pollara J, Tomaras GD, Haynes BF. 2017. Humoral and Innate Antiviral Immunity as Tools to Clear Persistent HIV Infection. J Infect Dis 215:S152-S159.
10. Burton DR, Hangartner L. 2016. Broadly Neutralizing Antibodies to HIV and Their Role in Vaccine Design. Annu Rev Immunol 34:635-59.
11. Haynes BF, Mascola JR. 2017. The quest for an antibody-based HIV vaccine. Immunol Rev 275:5-10.
12. Ward AB, Wilson IA. 2017. The HIV-1 envelope glycoprotein structure: nailing down a moving target. Immunol Rev 275:21-32.
13. Rudicell RS, Kwon YD, Ko SY, Pegu A, Louder MK, Georgiev IS, Wu X, Zhu J, Boyington JC, Chen X, Shi W, Yang ZY, Doria-Rose NA, McKee K, O'Dell S, Schmidt SD, Chuang GY, Druz A, Soto C, Yang Y, Zhang B, Zhou T, Todd JP, Lloyd KE, Eudailey J, Roberts KE, Donald BR, Bailer RT, Ledgerwood J, Program NCS, Mullikin JC, Shapiro L, Koup RA, Graham BS, Nason MC, Connors M, Haynes BF, Rao SS, Roederer M, Kwong PD, Mascola JR, Nabel GJ. 2014. Enhanced potency of a broadly neutralizing HIV-1 antibody in vitro improves protection against lentiviral infection in vivo. J Virol 88:12669-82.
14. Wu X, Yang ZY, Li Y, Hogerkorp CM, Schief WR, Seaman MS, Zhou T, Schmidt SD, Wu L, Xu L, Longo NS, McKee K, O'Dell S, Louder MK, Wycuff DL, Feng Y,

Nason M, Doria-Rose N, Connors M, Kwong PD, Roederer M, Wyatt RT, Nabel GJ, Mascola JR. 2010. Rational design of envelope identifies broadly neutralizing human monoclonal antibodies to HIV-1. Science 329:856-61.

15. Scheid JF, Mouquet H, Ueberheide B, Diskin R, Klein F, Oliveira TY, Pietzsch J, Fenyo D, Abadir A, Velinzon K, Hurley A, Myung S, Boulad F, Poignard P, Burton DR, Pereyra F, Ho DD, Walker BD, Seaman MS, Bjorkman PJ, Chait BT, Nussenzweig MC. 2011. Sequence and structural convergence of broad and potent HIV antibodies that mimic CD4 binding. Science 333:1633-7.

16. Huang J, Ofek G, Laub L, Louder MK, Doria-Rose NA, Longo NS, Imamichi H, Bailer RT, Chakrabarti B, Sharma SK, Alam SM, Wang T, Yang Y, Zhang B, Migueles SA, Wyatt R, Haynes BF, Kwong PD, Mascola JR, Connors M. 2012. Broad and potent neutralization of HIV-1 by a gp41-specific human antibody. Nature 491:406-12.

17. Huang J, Kang BH, Ishida E, Zhou T, Griesman T, Sheng Z, Wu F, Doria-Rose NA, Zhang B, McKee K, O'Dell S, Chuang GY, Druz A, Georgiev IS, Schramm CA, Zheng A, Joyce MG, Asokan M, Ransier A, Darko S, Migueles SA, Bailer RT, Louder MK, Alam SM, Parks R, Kelsoe G, Von Holle T, Haynes BF, Douek DC, Hirsch V, Seaman MS, Shapiro L, Mascola JR, Kwong PD, Connors M. 2016. Identification of a CD4-Binding-Site Antibody to HIV that Evolved Near-Pan Neutralization Breadth. Immunity 45:1108-1121.

18. Sok D, van Gils MJ, Pauthner M, Julien JP, Saye-Francisco KL, Hsueh J, Briney B, Lee JH, Le KM, Lee PS, Hua Y, Seaman MS, Moore JP, Ward AB, Wilson IA, Sanders RW, Burton DR. 2014. Recombinant HIV envelope trimer selects for quaternary-dependent antibodies targeting the trimer apex. Proc Natl Acad Sci U S A 111:17624-9.

19. Walker LM, Phogat SK, Chan-Hui PY, Wagner D, Phung P, Goss JL, Wrin T, Simek MD, Fling S, Mitcham JL, Lehrman JK, Priddy FH, Olsen OA, Frey SM, Hammond PW, Protocol GPI, Kaminsky S, Zamb T, Moyle M, Koff WC, Poignard P, Burton DR. 2009. Broad and potent neutralizing antibodies from an African donor reveal a new HIV-1 vaccine target. Science 326:285-9.

20. Walker LM, Huber M, Doores KJ, Falkowska E, Pejchal R, Julien JP, Wang SK, Ramos A, Chan-Hui PY, Moyle M, Mitcham JL, Hammond PW, Olsen OA, Phung P, Fling S, Wong CH, Phogat S, Wrin T, Simek MD, Protocol GPI, Koff WC, Wilson IA, Burton DR, Poignard P. 2011. Broad neutralization coverage of HIV by multiple highly potent antibodies. Nature 477:466-70.

21. Mouquet H, Scharf L, Euler Z, Liu Y, Eden C, Scheid JF, Halper-Stromberg A, Gnanapragasam PN, Spencer DI, Seaman MS, Schuitemaker H, Feizi T, Nussenzweig MC, Bjorkman PJ. 2012. Complex-type N-glycan recognition by potent broadly neutralizing HIV antibodies. Proc Natl Acad Sci U S A 109:E3268-77.

22. Doria-Rose NA, Bhiman JN, Roark RS, Schramm CA, Gorman J, Chuang GY, Pancera M, Cale EM, Ernandes MJ, Louder MK, Asokan M, Bailer RT, Druz A, Fraschilla IR, Garrett NJ, Jarosinski M, Lynch RM, McKee K, O'Dell S, Pegu A, Schmidt SD, Staupe RP, Sutton MS, Wang K, Wibmer CK, Haynes BF, Abdool-Karim S, Shapiro L, Kwong PD, Moore PL, Morris L, Mascola JR. 2015. New

Member of the V1V2-Directed CAP256-VRC26 Lineage That Shows Increased Breadth and Exceptional Potency. J Virol 90:76-91.

23. Bhiman JN, Lynch RM. 2017. Broadly Neutralizing Antibodies as Treatment: Effects on Virus and Immune System. Curr HIV/AIDS Rep 14:54-62.

24. Wibmer CK, Moore PL, Morris L. 2015. HIV broadly neutralizing antibody targets. Curr Opin HIV AIDS 10:135-43.

25. Wu X, Kong XP. 2016. Antigenic landscape of the HIV-1 envelope and new immunological concepts defined by HIV-1 broadly neutralizing antibodies. Curr Opin Immunol 42:56-64.

26. McCoy LE, Burton DR. 2017. Identification and specificity of broadly neutralizing antibodies against HIV. Immunol Rev 275:11-20.

27. Caskey M, Klein F, Lorenzi JC, Seaman MS, West AP, Jr., Buckley N, Kremer G, Nogueira L, Braunschweig M, Scheid JF, Horwitz JA, Shimeliovich I, Ben-Avraham S, Witmer-Pack M, Platten M, Lehmann C, Burke LA, Hawthorne T, Gorelick RJ, Walker BD, Keler T, Gulick RM, Fatkenheuer G, Schlesinger SJ, Nussenzweig MC. 2015. Viraemia suppressed in HIV-1-infected humans by broadly neutralizing antibody 3BNC117. Nature 522:487-91.

28. Caskey M, Schoofs T, Gruell H, Settler A, Karagounis T, Kreider EF, Murrell B, Pfeifer N, Nogueira L, Oliveira TY, Learn GH, Cohen YZ, Lehmann C, Gillor D, Shimeliovich I, Unson-O'Brien C, Weiland D, Robles A, Kummerle T, Wyen C, Levin R, Witmer-Pack M, Eren K, Ignacio C, Kiss S, West AP, Jr., Mouquet H, Zingman BS, Gulick RM, Keler T, Bjorkman PJ, Seaman MS, Hahn BH, Fatkenheuer G, Schlesinger SJ, Nussenzweig MC, Klein F. 2017. Antibody 10-1074 suppresses viremia in HIV-1-infected individuals. Nat Med 23:185-191.

29. Lynch RM, Boritz E, Coates EE, DeZure A, Madden P, Costner P, Enama ME, Plummer S, Holman L, Hendel CS, Gordon I, Casazza J, Conan-Cibotti M, Migueles SA, Tressler R, Bailer RT, McDermott A, Narpala S, O'Dell S, Wolf G, Lifson JD, Freemire BA, Gorelick RJ, Pandey JP, Mohan S, Chomont N, Fromentin R, Chun TW, Fauci AS, Schwartz RM, Koup RA, Douek DC, Hu Z, Capparelli E, Graham BS, Mascola JR, Ledgerwood JE, Team VRCS. 2015. Virologic effects of broadly neutralizing antibody VRC01 administration during chronic HIV-1 infection. Sci Transl Med 7:319ra206.

30. Bar KJ, Sneller MC, Harrison LJ, Justement JS, Overton ET, Petrone ME, Salantes DB, Seamon CA, Scheinfeld B, Kwan RW, Learn GH, Proschan MA, Kreider EF, Blazkova J, Bardsley M, Refsland EW, Messer M, Clarridge KE, Tustin NB, Madden PJ, Oden K, O'Dell SJ, Jarocki B, Shiakolas AR, Tressler RL, Doria-Rose NA, Bailer RT, Ledgerwood JE, Capparelli EV, Lynch RM, Graham BS, Moir S, Koup RA, Mascola JR, Hoxie JA, Fauci AS, Tebas P, Chun TW. 2016. Effect of HIV Antibody VRC01 on Viral Rebound after Treatment Interruption. N Engl J Med 375:2037-2050.

31. Scheid JF, Horwitz JA, Bar-On Y, Kreider EF, Lu CL, Lorenzi JC, Feldmann A, Braunschweig M, Nogueira L, Oliveira T, Shimeliovich I, Patel R, Burke L, Cohen YZ, Hadrigan S, Settler A, Witmer-Pack M, West AP, Jr., Juelg B, Keler T, Hawthorne T, Zingman B, Gulick RM, Pfeifer N, Learn GH, Seaman MS, Bjorkman PJ, Klein F, Schlesinger SJ, Walker BD, Hahn BH, Nussenzweig MC,

907 Caskey M. 2016. HIV-1 antibody 3BNC117 suppresses viral rebound in
908 humans during treatment interruption. Nature 535:556-60.
909 32. Bruel T, Guivel-Benhassine F, Lorin V, Lortat-Jacob H, Baleux F, Bourdic K,
910 Noel N, Lambotte O, Mouquet H, Schwartz O. 2017. Lack of ADCC Breadth of
911 Human Nonneutralizing Anti-HIV-1 Antibodies. J Virol 91.
912 33. von Bredow B, Arias JF, Heyer LN, Gardner MR, Farzan M, Rakasz EG, Evans
913 DT. 2015. Envelope Glycoprotein Internalization Protects Human and Simian
914 Immunodeficiency Virus-Infected Cells from Antibody-Dependent Cell-
915 Mediated Cytotoxicity. J Virol 89:10648-55.
916 34. von Bredow B, Arias JF, Heyer LN, Moldt B, Le K, Robinson JE, Zolla-Pazner S,
917 Burton DR, Evans DT. 2016. Comparison of Antibody-Dependent Cell-
918 Mediated Cytotoxicity and Virus Neutralization by HIV-1 Env-Specific
919 Monoclonal Antibodies. J Virol 90:6127-39.
920 35. Veillette M, Coutu M, Richard J, Batraville LA, Dagher O, Bernard N, Tremblay
921 C, Kaufmann DE, Roger M, Finzi A. 2015. The HIV-1 gp120 CD4-bound
922 conformation is preferentially targeted by antibody-dependent cellular
923 cytotoxicity-mediating antibodies in sera from HIV-1-infected individuals. J
924 Virol 89:545-51.
925 36. Decker JM, Bibollet-Ruche F, Wei X, Wang S, Levy DN, Wang W, Delaporte E,
926 Peeters M, Derdeyn CA, Allen S, Hunter E, Saag MS, Hoxie JA, Hahn BH, Kwong
927 PD, Robinson JE, Shaw GM. 2005. Antigenic conservation and
928 immunogenicity of the HIV coreceptor binding site. J Exp Med 201:1407-19.
929 37. Richard J, Veillette M, Brassard N, Iyer SS, Roger M, Martin L, Pazgier M,
930 Schon A, Freire E, Routy JP, Smith AB, 3rd, Park J, Jones DM, Courter JR,
931 Melillo BN, Kaufmann DE, Hahn BH, Permar SR, Haynes BF, Madani N,
932 Sodroski JG, Finzi A. 2015. CD4 mimetics sensitize HIV-1-infected cells to
933 ADCC. Proc Natl Acad Sci U S A 112:E2687-94.
934 38. Lee WS, Richard J, Lichtfuss M, Smith AB, 3rd, Park J, Courter JR, Melillo BN,
935 Sodroski JG, Kaufmann DE, Finzi A, Parsons MS, Kent SJ. 2015. Antibody-
936 Dependent Cellular Cytotoxicity against Reactivated HIV-1-Infected Cells. J
937 Virol 90:2021-30.
938 39. Boesch AW, Brown EP, Ackerman ME. 2015. The role of Fc receptors in HIV
939 prevention and therapy. Immunol Rev 268:296-310.
940 40. Mujib S, Liu J, Rahman A, Schwartz JA, Bonner P, Yue FY, Ostrowski MA. 2017.
941 Comprehensive Cross-Clade Characterization of Antibody-Mediated
942 Recognition, Complement-Mediated Lysis, and Cell-Mediated Cytotoxicity of
943 HIV-1 Envelope-Specific Antibodies toward Eradication of the HIV-1
944 Reservoir. J Virol 91.
945 41. Siliciano JD, Siliciano RF. 2005. Enhanced culture assay for detection and
946 quantitation of latently infected, resting CD4+ T-cells carrying replication-
947 competent virus in HIV-1-infected individuals. Methods Mol Biol 304:3-15.
948 42. Kong R, Louder MK, Wagh K, Bailer RT, deCamp A, Greene K, Gao H, Taft JD,
949 Gazumyan A, Liu C, Nussenzweig MC, Korber B, Montefiori DC, Mascola JR.
950 2015. Improving neutralization potency and breadth by combining broadly
951 reactive HIV-1 antibodies targeting major neutralization epitopes. J Virol
952 89:2659-71.

43. Wagh K, Bhattacharya T, Williamson C, Robles A, Bayne M, Garrity J, Rist M, Rademeyer C, Yoon H, Lapedes A, Gao H, Greene K, Louder MK, Kong R, Karim SA, Burton DR, Barouch DH, Nussenzweig MC, Mascola JR, Morris L, Montefiori DC, Korber B, Seaman MS. 2016. Optimal Combinations of Broadly Neutralizing Antibodies for Prevention and Treatment of HIV-1 Clade C Infection. PLoS Pathog 12:e1005520.

44. Georgiev IS, Doria-Rose NA, Zhou T, Kwon YD, Staupe RP, Moquin S, Chuang GY, Louder MK, Schmidt SD, Altae-Tran HR, Bailer RT, McKee K, Nason M, O'Dell S, Ofek G, Pancera M, Srivatsan S, Shapiro L, Connors M, Migueles SA, Morris L, Nishimura Y, Martin MA, Mascola JR, Kwong PD. 2013. Delineating antibody recognition in polyclonal sera from patterns of HIV-1 isolate neutralization. Science 340:751-6.

45. Kwon YD, Chuang GY, Zhang B, Bailer RT, Doria-Rose NA, Gindin TS, Lin B, Louder MK, McKee K, O'Dell S, Pegu A, Schmidt SD, Asokan M, Chen X, Choe M, Georgiev IS, Jin V, Pancera M, Rawi R, Wang K, Chaudhuri R, Kueltzo LA, Manceva SD, Todd JP, Scorpio DG, Kim M, Reinherz EL, Wagh K, Korber BM, Connors M, Shapiro L, Mascola JR, Kwong PD. 2018. Surface-Matrix Screening Identifies Semi-specific Interactions that Improve Potency of a Near Pan-reactive HIV-1-Neutralizing Antibody. Cell Rep 22:1798-1809.

46. Gong JH, Maki G, Klingemann HG. 1994. Characterization of a human cell line (NK-92) with phenotypical and functional characteristics of activated natural killer cells. Leukemia 8:652-8.

47. Jochems C, Hodge JW, Fantini M, Fujii R, Morillon YM, 2nd, Greiner JW, Padget MR, Tritsch SR, Tsang KY, Campbell KS, Klingemann H, Boissel L, Rabizadeh S, Soon-Shiong P, Schlom J. 2016. An NK cell line (haNK) expressing high levels of granzyme and engineered to express the high affinity CD16 allele. Oncotarget 7:86359-86373.

48. Collins KL, Chen BK, Kalams SA, Walker BD, Baltimore D. 1998. HIV-1 Nef protein protects infected primary cells against killing by cytotoxic T lymphocytes. Nature 391:397-401.

49. Apps R, Del Prete GQ, Chatterjee P, Lara A, Brumme ZL, Brockman MA, Neil S, Pickering S, Schneider DK, Piechocka-Trocha A, Walker BD, Thomas R, Shaw GM, Hahn BH, Keele BF, Lifson JD, Carrington M. 2016. HIV-1 Vpu Mediates HLA-C Downregulation. Cell Host Microbe 19:686-95.

50. Crise B, Buonocore L, Rose JK. 1990. CD4 is retained in the endoplasmic reticulum by the human immunodeficiency virus type 1 glycoprotein precursor. J Virol 64:5585-93.

51. Dalgleish AG, Beverley PC, Clapham PR, Crawford DH, Greaves MF, Weiss RA. 1984. The CD4 (T4) antigen is an essential component of the receptor for the AIDS retrovirus. Nature 312:763-7.

52. Garcia JV, Miller AD. 1991. Serine phosphorylation-independent downregulation of cell-surface CD4 by nef. Nature 350:508-11.

53. Willey RL, Maldarelli F, Martin MA, Strebel K. 1992. Human immunodeficiency virus type 1 Vpu protein regulates the formation of intracellular gp160-CD4 complexes. J Virol 66:226-34.

54. Veillette M, Desormeaux A, Medjahed H, Gharsallah NE, Coutu M, Baalwa J, Guan Y, Lewis G, Ferrari G, Hahn BH, Haynes BF, Robinson JE, Kaufmann DE, Bonsignori M, Sodroski J, Finzi A. 2014. Interaction with cellular CD4 exposes HIV-1 envelope epitopes targeted by antibody-dependent cell-mediated cytotoxicity. J Virol 88:2633-44.

55. Li Y, O'Dell S, Walker LM, Wu X, Guenaga J, Feng Y, Schmidt SD, McKee K, Louder MK, Ledgerwood JE, Graham BS, Haynes BF, Burton DR, Wyatt RT, Mascola JR. 2011. Mechanism of neutralization by the broadly neutralizing HIV-1 monoclonal antibody VRC01. J Virol 85:8954-67.

56. Louder MK, Sambor A, Chertova E, Hunte T, Barrett S, Ojong F, Sanders-Buell E, Zolla-Pazner S, McCutchan FE, Roser JD, Gabuzda D, Lifson JD, Mascola JR. 2005. HIV-1 envelope pseudotyped viral vectors and infectious molecular clones expressing the same envelope glycoprotein have a similar neutralization phenotype, but culture in peripheral blood mononuclear cells is associated with decreased neutralization sensitivity. Virology 339:226-38.

57. Mann AM, Rusert P, Berlinger L, Kuster H, Gunthard HF, Trkola A. 2009. HIV sensitivity to neutralization is determined by target and virus producer cell properties. AIDS 23:1659-67.

58. Cohen YZ, Lorenzi JCC, Seaman MS, Nogueira L, Schoofs T, Krassnig L, Butler A, Millard K, Fitzsimons T, Daniell X, Dizon JP, Shimeliovich I, Montefiori DC, Caskey M, Nussenzweig MC. 2018. Neutralizing Activity of Broadly Neutralizing Anti-HIV-1 Antibodies against Clade B Clinical Isolates Produced in Peripheral Blood Mononuclear Cells. J Virol 92.

59. Moore PL, Crooks ET, Porter L, Zhu P, Cayanan CS, Grise H, Corcoran P, Zwick MB, Franti M, Morris L, Roux KH, Burton DR, Binley JM. 2006. Nature of nonfunctional envelope proteins on the surface of human immunodeficiency virus type 1. J Virol 80:2515-28.

60. Horwitz JA, Bar-On Y, Lu CL, Fera D, Lockhart AAK, Lorenzi JCC, Nogueira L, Golijanin J, Scheid JF, Seaman MS, Gazumyan A, Zolla-Pazner S, Nussenzweig MC. 2017. Non-neutralizing Antibodies Alter the Course of HIV-1 Infection In Vivo. Cell 170:637-648 e10.

61. Scharf L, Wang H, Gao H, Chen S, McDowall AW, Bjorkman PJ. 2015. Broadly Neutralizing Antibody 8ANC195 Recognizes Closed and Open States of HIV-1 Env. Cell 162:1379-90.

62. Blattner C, Lee JH, Sliepen K, Derking R, Falkowska E, de la Pena AT, Cupo A, Julien JP, van Gils M, Lee PS, Peng W, Paulson JC, Poignard P, Burton DR, Moore JP, Sanders RW, Wilson IA, Ward AB. 2014. Structural delineation of a quaternary, cleavage-dependent epitope at the gp41-gp120 interface on intact HIV-1 Env trimers. Immunity 40:669-80.

63. Lorenzi JC, Cohen YZ, Cohn LB, Kreider EF, Barton JP, Learn GH, Oliveira T, Lavine CL, Horwitz JA, Settler A, Jankovic M, Seaman MS, Chakraborty AK, Hahn BH, Caskey M, Nussenzweig MC. 2016. Paired quantitative and qualitative assessment of the replication-competent HIV-1 reservoir and comparison with integrated proviral DNA. Proc Natl Acad Sci U S A 113:E7908-E7916.

64. Seaman MS, Janes H, Hawkins N, Grandpre LE, Devoy C, Giri A, Coffey RT, Harris L, Wood B, Daniels MG, Bhattacharya T, Lapedes A, Polonis VR, McCutchan FE, Gilbert PB, Self SG, Korber BT, Montefiori DC, Mascola JR. 2010. Tiered categorization of a diverse panel of HIV-1 Env pseudoviruses for assessment of neutralizing antibodies. J Virol 84:1439-52.

65. Salazar-Gonzalez JF, Salazar MG, Keele BF, Learn GH, Giorgi EE, Li H, Decker JM, Wang S, Baalwa J, Kraus MH, Parrish NF, Shaw KS, Guffey MB, Bar KJ, Davis KL, Ochsenbauer-Jambor C, Kappes JC, Saag MS, Cohen MS, Mulenga J, Derdeyn CA, Allen S, Hunter E, Markowitz M, Hraber P, Perelson AS, Bhattacharya T, Haynes BF, Korber BT, Hahn BH, Shaw GM. 2009. Genetic identity, biological phenotype, and evolutionary pathways of transmitted/founder viruses in acute and early HIV-1 infection. J Exp Med 206:1273-89.

66. Raska M, Takahashi K, Czernekova L, Zachova K, Hall S, Moldoveanu Z, Elliott MC, Wilson L, Brown R, Jancova D, Barnes S, Vrbkova J, Tomana M, Smith PD, Mestecky J, Renfrow MB, Novak J. 2010. Glycosylation patterns of HIV-1 gp120 depend on the type of expressing cells and affect antibody recognition. J Biol Chem 285:20860-9.

67. Sarzotti-Kelsoe M, Bailer RT, Turk E, Lin CL, Bilska M, Greene KM, Gao H, Todd CA, Ozaki DA, Seaman MS, Mascola JR, Montefiori DC. 2014. Optimization and validation of the TZM-bl assay for standardized assessments of neutralizing antibodies against HIV-1. J Immunol Methods 409:131-46.

68. Han KP, Zhu X, Liu B, Jeng E, Kong L, Yovandich JL, Vyas VV, Marcus WD, Chavaillaz PA, Romero CA, Rhode PR, Wong HC. 2011. IL-15:IL-15 receptor alpha superagonist complex: high-level co-expression in recombinant mammalian cells, purification and characterization. Cytokine 56:804-10.

69. Wagner JA, Rosario M, Romee R, Berrien-Elliott MM, Schneider SE, Leong JW, Sullivan RP, Jewell BA, Becker-Hapak M, Schappe T, Abdel-Latif S, Ireland AR, Jaishankar D, King JA, Vij R, Clement D, Goodridge J, Malmberg KJ, Wong HC, Fehniger TA. 2017. CD56bright NK cells exhibit potent antitumor responses following IL-15 priming. J Clin Invest 127:4042-4058.

Figure Legends

Figure 1. Schematic for paired assessment of virus neutralization and infected cell binding with reactivated reservoir viruses. Quantitative Viral Outgrowth Assays (QVOA) were performed using $CD4^+$ T-cells from ARV-suppressed study participants. Virus was isolated from HIV-$p24^+$ wells at a dilution where < 50% of wells were positive. A portion of the supernatants from each of these wells was used directly to assess virus neutralization using a TZM-bl assay. Another portion was used to infect activated primary $CD4^+$ T-cells. Binding of bNAbs to these infected cells was assessed by flow cytometry, co-staining with CD3, CD4 and HIV-Gag to identify infected cells.

Figure 2. Breadth and potency of neutralization of a panel of bNAbs against reactivated reservoir viruses (A) Representative neutralization curves against virus isolates #1 & #3 from study participant OM5162. Each graph represents antibodies targeting similar epitopes against one virus, and each curve represents results from one bNAb. (B) The half maximal inhibitory concentration (IC_{50}) and (C) IC_{80} are shown in heat-maps. The lower the antibody concentration, the more sensitive the reservoir virus is to a specific bNAb (bNAbs were shown by binding epitope classes; HIV-IG, positive control antibody; 4G2-Hu, negative control antibody). The geometric mean concentration against all 36 (or 35) reservoir viruses tested was calculated. Numbers in Cyan bold are those where a single bNAb provided coverage of each of the viral isolates tested from a

given participant. (D) Heat-map showing neutralization coverage of antibody combinations. Shown are the % of viral isolates that were neutralized by at least one antibody in the indicated combinations using an IC_{80} cut off of 10 μg/ml.

Figure 3. Breadth, potency and functional consequences of binding of a panel of bNAbs against reactivated reservoir viruses. (A) Representative flow plots showing bNAb binding to cells infected with reservoir viruses, gated on live/$CD3^+$ cell populations. For each bNAb/virus combination we calculated a median intensity fluorescence (MFI) ratio, defined as MFI of bnAbs in HIV infected cell population (Gag^+) / MFI of bnAbs in HIV uninfected cell population (Gag^-). The displayed plots provide an example intra-participant diversity in bNAb binding to different viral isolates. (B) Heat-map showing binding of bNAbs at 5 μg/ml to the indicated viral isolates. The numbers given are MFI ratios, with higher values indicating higher levels of binding. (C) Heat-map showing binding of each bNAb to infected cells when tested at its neutralization geometric mean IC_{80} neutralization concentration. (D) Heat-map showing binding coverage of single bNAbs and two bNAb combinations. The breadth of coverage of antibody combinations was defined based on having at least one of the two bNAbs bind with an MFI ratio > 2. (E) Representative flow cytometry plots from ADCC assays, sampled after the 7 hour co-culture periods and gated on live/$CD3^+$ cell populations. The no NK cell conditions (top row) show populations of HIV-infected cells (Gag^+) that also stain positive for the bNAb PGT121 when added. The addition of either haNK cells (middle row) or primary NK cells (bottom row)

resulted in substantial reductions in HIV-infected cell populations, which was generally enhanced by the addition of bNAbs. For the conditions with PGT121, the killing of HIV-infected cells can also be observed in the elimination of cells staining positive for PGT121 in the conditions with NK cells. (F) Correlations between killing frequency (%) and infected cell binding (left panel), and ADCC (%) and infected cell binding (right panel). Both correlations were tested with 2 reservoir viruses combined with 9 bNAbs and the A32 antibody. Each virus/bNAb combination is indicated by a dot, and each color represents one effector cell type, red - haNK cells, green - primary NK cells from the PBMCs of a HIV-negative donor (allogeneic). Correlation coefficients (r) and statistical significance (p) were calculated using Spearman's Rank-Order Correlation.

Figure 4. Comparisons between bNAb binding to early (Gag^+CD4^+) versus late (Gag^+CD4^-) HIV-infected cell populations. Gag^+CD4^- population represents the specific binding to HIV Env. (A) Representative flow cytometry plots gated on lymphocytes/live/$CD3^+$ (left panels), and on lymphocytes/live/$CD3^+$/HIV-Gag^+ (right panels) showing differential bNAb binding to $CD4^+$ (early infected) and $CD4^-$ (late infected) populations. The results show that for 3BNC117, 10-1074 and PG9 most of the bNAb binding to infected cells (Gag^+) occurs with the $CD4^-$ population. In contrast, for 10E8v4-V5R-100cF $CD4^+$ T-cells are bound at similar or slightly higher levels than $CD4^-$ T-cells (within the Gag^+ population). (B) Summary data for the analysis represented in panel A, showing paired comparisons of MFI ratios between $CD4^+$ and $CD4^-$ populations.

MFI ratio is defined as (MFI of bNAbs in $Gag^{+}CD4^{+}$)/ (MFI of bNAbs in Gag^{-}) (green dots) or (MFI of bNAbs in $Gag^{+}CD4^{-}$)/ (MFI of bNAbs in Gag^{-}) (red dots). The numbers indicate fold differences (mean of $Gag^{+}CD4^{-}$ MFI ratio)/ (mean of $Gag^{+}CD4^{+}$ MFI ratio) (Wilcoxon matched-pairs signed rank test, **** $p<0.0001$, ** $p<0.01$).

Figure 5. Correlations between virus neutralization and paired late-infected cell binding at 5 µg/ml bNAb concentrations. Shown are correlations between IC_{80} virus neutralization values and binding to late-infected cells ($Gag^{+}CD4^{-}$) using a 5 µg/ml concentration for each antibody. (A) Correlation for all antibodies tested together. (B) Correlations for each bNAb tested independently. Each virus/bNAb combination is indicated by a circle, and each color represents one study participant. Correlations were analyzed by Spearman correlation coefficient (r), with statistical significance highlighted in red letters.

Supplementary figure legends

sFig1. Heat-map of bNAb binding to late-infected (Gag^+CD4^-) cell populations at geometric mean IC_{80} neutralization concentrations. Binding assay were performed with individual geometric mean neutralization IC_{80} concentrations for each bNAb. The numbers indicate MFI ratios of the Gag^+CD4^- population (late infected) / Gag^- population (uninfected). Thus a higher value represents a higher level of specific bNAb binding.

sFig2. Correlations between virus neutralization and bNAb binding to total infected population (all Gag^+) when tested at 5 µg/ml. Shown are correlations between IC_{80} virus neutralization values and binding to HIV-infected cells (total Gag^+, thus groups early and late infection) with each bNAb tested at 5 µg/ml (A) Correlation for all antibodies tested together. (B) Correlations for each bNAb tested independently. Each virus/bNAb combination is indicated by a circle, and each color represents one study participant. Correlations were analyzed by Spearman correlation coefficient (r), with statistical significance highlighted in red lettering.

sFig3. Correlations between virus neutralization and bNAb binding to late-infected populations (all $Gag^{+/}CD4^-$) when tested at neutralization geometric mean IC_{80} concentrations. Shown are correlations between IC_{80} virus neutralization values and binding to late-infected cells ($Gag^{+/}CD4^-$) with each

bNAb tested at its individual geometric mean neutralization IC_{80} concentration (A) Correlation for all antibodies tested together. (B) Correlations for each bNAb tested independently. Each virus/bNAb combination is indicated by a circle, and each color represents one study participant. Correlations were analyzed by Spearman correlation coefficient (r), with statistical significance highlighted in red lettering.

sFig4. Correlations between virus neutralization and bNAb binding to total infected population (all Gag^+) when tested at geometric mean neutralization IC_{80} concentrations. Shown are correlations between IC_{80} virus neutralization values and binding to HIV-infected cells (total Gag^+, thus groups early and late infection) with each bNAb tested at individual neutralization geometric mean IC_{80} concentrations (A) Correlation for all antibodies tested together. (B) Correlations for each bNAb tested independently. Each virus/bNAb combination is indicated by a circle, and each color represents one study participant. Correlations were analyzed by Spearman correlation coefficient (r), with statistical significance highlighted in red lettering.

Table 1. Patient clinical information

Participant ID	Age	Sex	Viral Load (copies/ml)	CD4 Count	HIV Clade	Time to Initiation of ART (month)	Duration of ART (years)	IUPM
OM5148	47	Male	NA	$0.733x10^9$/L	B	57	10	1.02
OM5334	33	Male	NA	$0.812x10^9$/L	B	2	3	1.67
OM5001	43	Male	42	$0.540x10^9$/L	B	14	9	10.46
OM5365	56	Male	NA	$0.624X10^9$/L	E, B	18	25	0.421
CIRC0196	56	Male	NA	$0.679x10^9$/L	B	75	3	0.486
OM5346	48	Male	NA	$1.182x10^9$/L	B	1.5	5	0.27
OM5162	53	Male	NA	$0.478X10^9$/L	B	3.5	14	0.65
OM5267	29	Male	NA	$0.429X10^9$/L	B	4.5	3	2.344

Fig. 1

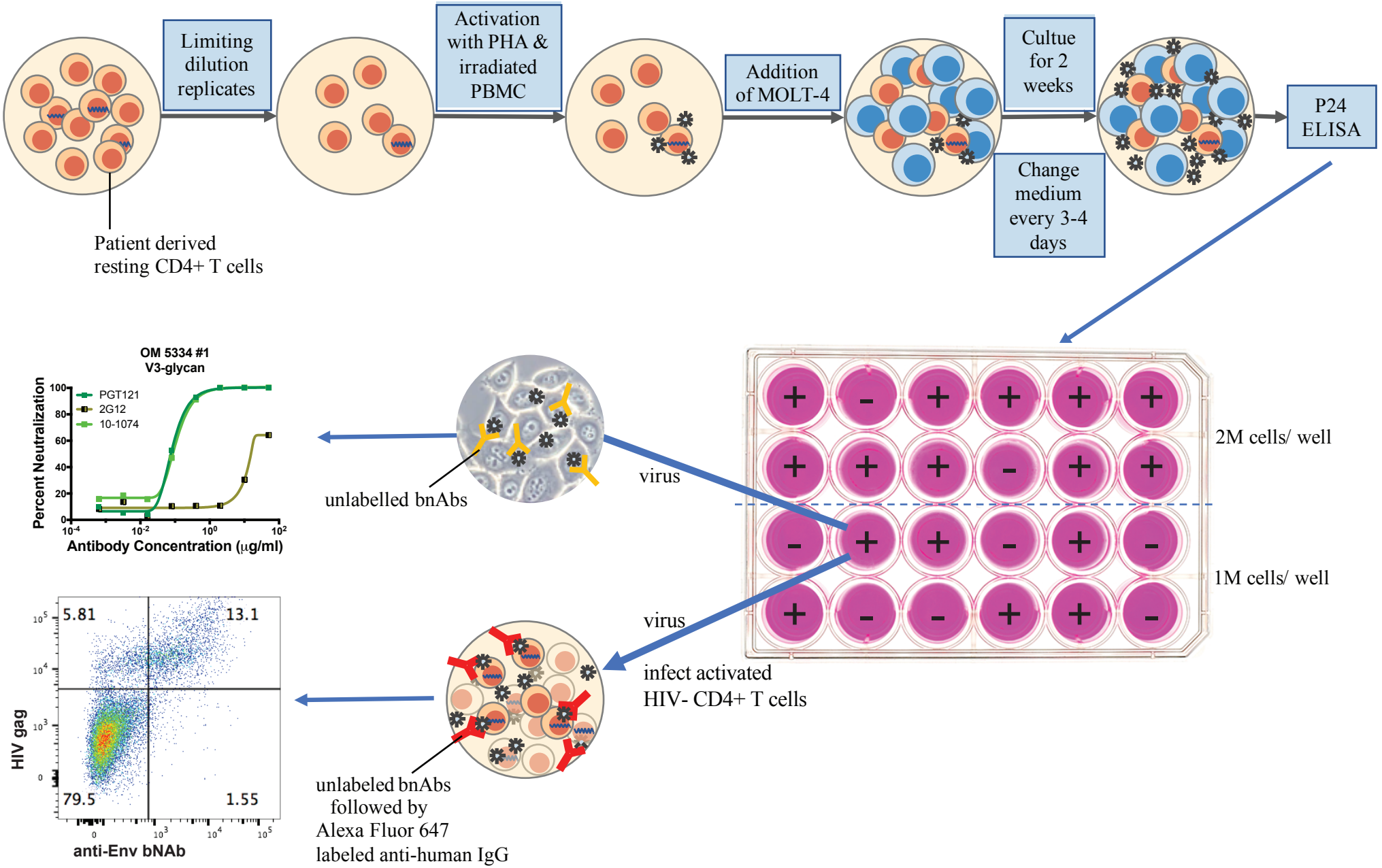
Limiting dilution replicates
Activation with PHA & irradiated PBMC
Addition of MOLT-4
Cultue for 2 weeks
Change medium every 3-4 days
P24 ELISA
Patient derived resting CD4+ T cells
OM 5334 #1
V3-glycan
PGT121
2G12
10-1074
Percent Neutralization
Antibody Concentration (μg/ml)
unlabelled bnAbs
virus
2M cells/ well
1M cells/ well
virus
infect activated HIV- CD4+ T cells
5.81
13.1
79.5
1.55
HIV gag
anti-Env bNAb
unlabeled bnAbs followed by Alexa Fluor 647 labeled anti-human IgG

Fig. 2

A

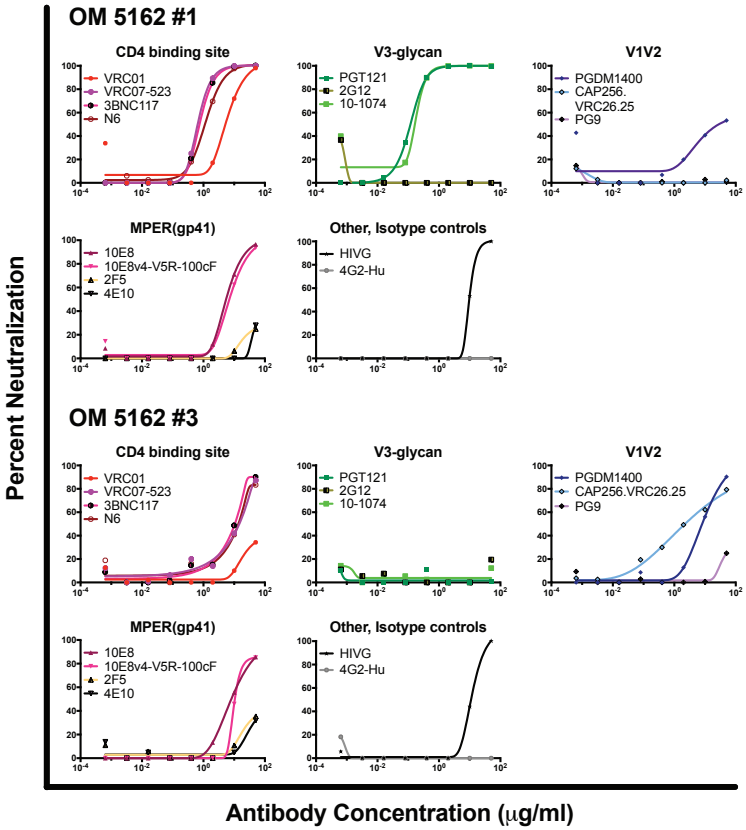

B *IC50 μg/ml*

	CD4 Binding Site				V3 Glycan			V1/V2			MPER (gp41)					
	VRC01	VRC07-523	3BNC117	N6	PGT121	2G12	10-1074	PGDM1400	CAP256. VRC26.25	PG9	10E8	10E8v4-V5R-100cF	2F5	4E10	HIVG	4G2-Hu
OM5148 #1	13.4	6.96	2.99	2.42	0.107	>50	0.102	20.1	>50	>50	>50	41.9	>50	>50	12.9	>50
OM5148 #2	9.27	3.27	1.47	2.03	0.259	>50	0.196	1.32	>50	>50	>50	25.1	>50	>50	10.0	>50
OM5148 #3	36.8	8.77	5.84	7.59	0.968	>50	1.50	>50	>50	>50	>50	>50	>50	>50	10.3	>50
OM5148 #5	0.259	3.27	1.47	2.03	9.27	>50	0.20	1.32	>50	>50	>50	25.1	>50	>50	10.0	>50
OM5148 #6	15.5	4.00	1.81	2.63	0.195	30.7	0.224	2.77	15.5	30.7	0.224	2.77	>50	39.9	7.28	>50
OM5334 #1	14.4	3.95	8.63	2.35	0.075	15.5	0.086	1.81	42.6	0.298	10.2	3.58	>50	>50	7.76	>50
OM5334 #6	23.0	6.25	13.6	4.79	23.0	6.25	13.6	4.79	>50	1.33	11.8	3.99	>50	49.6	8.56	>50
OM5334 #7	39.1	13.7	33.7	9.16	0.241	>50	0.311	8.31	>50	3.03	35.1	9.67	>50	>50	10.4	>50
OM5334 #10	15.5	5.02	12.9	3.71	0.059	>50	0.101	4.18	>50	0.360	12.8	5.47	>50	>50	8.22	>50
OM5334 #11	34.3	8.01	21.1	5.66	0.109	>50	0.222	7.74	>50	1.04	12.9	9.00	>50	>50	12.2	>50
OM5001 #3	3.63	0.751	1.11	0.458	0.259	>50	1.34	4.00	>50	0.184	1.47	1.23	>50	>50	9.49	>50
OM5001 #7	4.24	1.01	1.43	1.02	0.098	>50	1.69	>50	>50	0.278	3.98	1.26	22.8	>50	4.29	>50
OM5001 #9	5.24	0.703	1.09	0.849	0.076	>50	0.137	>50	>50	0.507	6.69	3.19	>50	>50	7.41	>50
OM5001 #10	3.14	0.544	0.620	0.653	0.156	>50	0.116	1.79	>50	0.096	0.137	0.05	2.43	7.22	6.27	>50
OM5001 #11	4.45	0.576	0.738	1.10	0.160	>50	0.088	2.02	>50	0.110	0.611	0.297	6.22	13.2	9.47	>50
OM5365 #1	16.4	2.84	1.42	4.01	0.158	12.6	0.105	0.764	>50	0.340	5.78	2.92	>50	>50	8.20	>50
OM5365 #2	6.79	1.88	1.23	2.22	0.314	>50	0.691	4.520	>50	0.489	1.71	0.851	16.3	15.5	8.34	>50
OM5365 #4	ND	ND	0.671	ND	ND	ND	0.19	ND	ND	0.522	ND	ND	ND	ND	8.43	ND
CIRC0196 #2	9.92	1.95	0.920	1.34	>50	>50	>50	>50	>50	7.28	2.87	0.595	24.8	22.2	7.50	>50
CIRC0196 #3	>50	13.5	12.1	9.97	>50	>50	>50	>50	>50	>50	4.22	0.958	18.5	45.2	6.98	>50
CIRC0196 #4	8.25	1.55	0.990	1.28	>50	>50	>50	>50	>50	1.35	9.15	3.08	20.9	30.8	7.23	>50
CIRC0196 #5	45.8	6.45	5.08	6.00	>50	>50	>50	>50	>50	>50	8.56	3.32	>50	>50	5.43	>50
CIRC0196 #6	3.54	0.877	0.465	0.892	>50	>50	>50	>50	>50	0.604	6.56	1.14	>50	22.1	5.11	>50
OM5346 #2	>50	0.384	1.28	0.115	18.5	>50	>50	0.013	0.0006	0.133	1.32	0.667	37.2	41.4	3.12	>50
OM5346 #3	4.49	1.57	>50	>50	8.75	28.0	0.679	>50	>50	>50	10.8	7.94	>50	>50	4.45	>50
OM5346 #4	14.1	0.224	0.415	0.080	>50	>50	>50	0.008	0.0006	0.159	0.484	0.101	6.24	8.91	4.19	>50
OM5346 #5	6.78	1.22	0.705	1.05	>50	>50	0.119	>50	1.15	>50	3.36	2.02	32.6	>50	6.08	>50
OM5162 #1	5.19	0.6	0.7	1.1	0.118	>50	0.165	27.9	>50	>50	5.47	6.99	>50	>50	9.66	>50
OM5162 #3	>50	14.7	10.5	13.7	>50	>50	>50	8.07	2.23	>50	8.07	10.5	>50	>50	11.0	>50
OM5162 #11	>50	11.0	9.05	20.5	>50	>50	>50	10.8	0.8	>50	14.9	9.63	>50	>50	10.5	>50
OM5162 #13	>50	9.62	9.87	16.7	>50	>50	>50	9.82	3.06	>50	11.4	4.94	>50	>50	8.03	>50
OM5162 #15	>50	21.9	10.1	16.9	>50	>50	>50	9.55	0.6	>50	24.6	14.5	>50	>50	9.52	>50
OM5267 #1	43.8	0.701	0.212	0.431	0.128	35.7	4.98	>50	>50	>50	5.27	2.89	4.10	15.5	0.102	>50
OM5267 #4	>50	2.66	0.740	1.98	0.083	35.3	0.208	>50	>50	>50	1.12	1.06	13.6	23.1	7.24	>50
OM5267 #5	1.98	0.323	0.085	0.146	0.083	15.5	0.067	>50	>50	>50	2.59	1.04	36.3	28.6	3.96	>50
OM5267 #8	>50	11.6	4.61	4.03	0.144	>50	0.148	>50	>50	>50	5.00	3.14	34.5	38.1	3.76	>50
Detectable neutralized (%)	77%	100%	97%	97%	69%	23%	69%	60%	26%	53%	89%	97%	40%	43%		
Geo Mean of neutralized virus (<50μg/ml)	8.9	2.6	2.1	2.1	0.3	19.4	0.3	2.5	0.5	0.6	4.1	2.7	15.0	23.1		

IC (μg/ml): >50 | 10-50 | 1-10 | 0.1-1 | <0.1 | ND = not done

C *IC80 μg/ml*

	CD4 Binding Site				V3 Glycan			V1/V2			MPER (gp41)					
	VRC01	VRC07-523	3BNC117	N6	PGT121	2G12	10-1074	PGDM1400	CAP256. VRC26.25	PG9	10E8	10E8v4-V5R-100cF	2F5	4E10	HIVG	4G2-Hu
OM5148 #1	25.1	10.1	5.42	4.54	0.244	>50	0.223	>50	>50	>50	>50	>50	>50	>50	29.3	>50
OM5148 #2	21.3	6.19	2.00	3.69	0.485	>50	0.383	4.34	>50	>50	>50	>50	>50	>50	14.0	>50
OM5148 #3	48.9	16.8	9.05	11.2	1.49	>50	1.78	>50	>50	>50	>50	>50	>50	>50	28.5	>50
OM5148 #5	0.485	6.19	2.00	3.69	21.3	>50	0.383	4.34	>50	>50	>50	>50	>50	>50	14.0	>50
OM5148 #6	32.02	10.0	3.82	5.59	0.425	>50	0.447	7.30	32.0	>50	0.447	7.30	>50	>50	19.6	>50
OM5334 #1	35.4	10.1	25.8	6.29	0.174	>50	0.207	5.01	>50	1.61	17.2	11.7	>50	>50	11.9	>50
OM5334 #6	36.8	10.1	26.7	7.48	36.8	10.1	26.7	7.48	>50	7.83	26.8	13.0	>50	>50	13.6	>50
OM5334 #7	>50	26.0	46.3	17.3	0.412	>50	0.455	24.4	>50	37.3	>50	20.4	>50	>50	21.3	>50
OM5334 #10	32.5	13.7	26.5	8.41	0.145	>50	0.244	14.2	>50	1.57	38.3	17.6	>50	>50	14.5	>50
OM5334 #11	47.7	14.3	40.6	11.8	0.218	>50	0.371	20.1	>50	4.38	32.6	15.1	>50	>50	28.8	>50
OM5001 #3	10.4	1.83	2.16	1.86	0.556	>50	1.89	>50	>50	0.409	7.14	3.95	>50	>50	17.9	>50
OM5001 #7	13.7	2.22	3.53	4.32	0.391	>50	>50	>50	>50	0.790	14.3	7.87	>50	>50	11.4	>50
OM5001 #9	15.7	2.84	3.98	2.86	0.273	>50	0.481	>50	>50	>50	25.1	14.6	>50	>50	19.4	>50
OM5001 #10	8.59	1.60	2.05	2.36	0.553	>50	0.675	11.3	>50	0.323	1.09	0.595	26.1	49.2	13.0	>50
OM5001 #11	11.2	2.13	2.74	2.21	0.632	>50	0.290	18.1	>50	0.883	5.44	2.83	>50	>50	16.0	>50
OM5365 #1	>50	9.49	4.53	16.1	0.863	>50	0.317	2.12	>50	1.02	27.8	18.8	>50	>50	11.7	>50
OM5365 #2	26.1	5.17	3.97	6.77	1.05	>50	5.99	10.4	>50	2.08	11.6	5.58	>50	>50	12.1	>50
OM5365 #4	ND	ND	2.14	ND	ND	ND	0.896	ND	ND	2.40	ND	ND	ND	ND	17.0	ND
CIRC0196 #2	21.8	5.39	2.48	4.37	>50	>50	>50	>50	>50	>50	15.9	5.50	>50	>50	18.5	>50
CIRC0196 #3	>50	37.2	38.2	37.4	>50	>50	>50	>50	>50	>50	18.5	9.83	>50	>50	17.7	>50
CIRC0196 #4	26.5	4.78	2.03	4.84	>50	>50	>50	>50	>50	>50	42.5	16.5	>50	>50	12.4	>50
CIRC0196 #5	>50	11.5	18.1	10.2	>50	>50	>50	>50	>50	>50	29.6	11.8	>50	>50	15.2	>50
CIRC0196 #6	10.9	2.49	1.45	1.89	>50	>50	>50	>50	>50	>50	15.1	8.40	>50	>50	14.5	>50
OM5346 #2	>50	1.55	13.6	0.691	>50	>50	>50	0.083	0.0005	1.13	10.6	5.57	>50	>50	8.97	>50
OM5346 #3	13.1	4.53	>50	>50	>50	>50	2.67	>50	>50	>50	40.0	12.6	>50	>50	11.97	>50
OM5346 #4	>50	1.07	4.36	0.415	>50	>50	>50	0.041	0.0002	1.70	2.395	0.941	>50	>50	11.56	>50
OM5346 #5	25.1	3.20	1.85	3.20	0.137	>50	0.407	>50	>50	>50	15.3	9.46	>50	>50	16.84	>50
OM5162 #1	13.6	1.32	1.59	2.88	0.259	>50	0.288	>50	>50	>50	14.1	19.6	>50	>50	14.1	>50
OM5162 #3	>50	38.3	21.7	29.3	>50	>50	>50	26.9	>50	>50	32.9	21.4	>50	>50	21.0	>50
OM5162 #11	>50	>50	37.0	>50	>50	>50	>50	28.5	>50	>50	>50	>50	>50	>50	25.3	>50
OM5162 #13	>50	>50	17.6	>50	>50	>50	>50	42.0	>50	>50	>50	25.3	>50	>50	13.8	>50
OM5162 #15	>50	>50	14.3	>50	>50	>50	>50	12.3	>50	>50	>50	46.9	>50	>50	12.2	>50
OM5267 #1	>50	1.75	0.765	1.30	0.478	>50	12.9	>50	>50	>50	27.5	14.1	11.5	>50	0.355	>50
OM5267 #4	>50	19.1	5.42	7.92	0.451	>50	0.704	>50	>50	>50	10.4	5.65	>50	>50	10.4	>50
OM5267 #5	5.75	0.903	0.336	0.695	0.287	46.4	0.236	>50	>50	>50	22.1	8.58	>50	>50	8.24	>50
OM5267 #8	>50	31.2	10.0	10.5	0.521	>50	0.549	>50	>50	>50	16.9	10.8	>50	>50	7.91	>50
Detectable neutralized (%)	63%	91%	97%	89%	66%	6%	67%	51%	9%	39%	77%	86%	6%	3%		
Geo Mean of neutralized virus (<50μg/ml)	16.7	5.7	5.8	4.6	0.6	21.7	0.7	6.3	0.0	1.8	13.7	9.3	17.3	49.2		

D Neutralization coverage of antibody combinations (IC_{80}≤10μg/ml)

		CD4 binding sites				V3-Glycan			V1/V2			MPER			
		VRC01	VRC07-523	3BNC117	N6	PGT121	2G12	10-1074	PGDM1400	CAP256. VRC26.25	PG9	10E8	10E8v4-V5R-100cF	2F5	4E10
CD4 binding site	VRC01	8%													
	VRC07-523	56%	56%												
	3BNC117	64%	69%	64%											
	N6	64%	69%	75%	64%										
V3-Glycar	PGT121	61%	78%	75%	78%	58%									
	2G12	8%	56%	64%	64%	58%	0%								
	10-1074	61%	81%	78%	83%	67%	61%	61%							
V1/V2	PGDM1400	28%	61%	72%	67%	69%	22%	69%	22%						
	CAP256. VRC26.25	14%	56%	67%	64%	64%	6%	67%	22%	6%					
	PG9	42%	69%	78%	72%	69%	36%	72%	44%	36%	36%				
MPER	10E8	19%	56%	64%	64%	61%	14%	64%	31%	17%	39%	14%			
	10E8v4-V5R-100cF	39%	61%	69%	67%	72%	39%	78%	53%	39%	56%	39%	39%		
	2F5	8%	56%	64%	64%	58%	0%	61%	22%	6%	36%	14%	39%	0%	
	4E10	8%	56%	64%	64%	58%	0%	61%	22%	6%	36%	14%	39%	0%	0%

Fig. 3

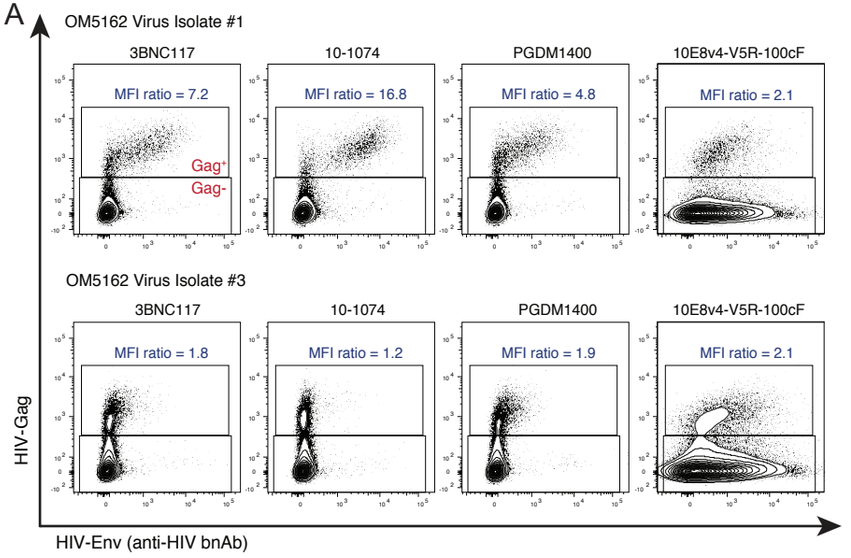

B **Each antibody used at 5μg/ml concentration**

	CD4 Binding Site				V3 Glycan			V1/V2			MPER (gp41)			
	VRC01	VRC07-523	3BNC117	N6	PGT121	2G12	10-1074	PGDM1400	CAP256.VRC26.25	PG9	10E8	10E8v4-V5R-100cF	2F5	4E10
OM5148 #1	1.7	1.1	2.4	1.5	2.7	5.8	7.8	3.4	1.3	2.9	1.6	1.8	1.4	1.1
OM5148 #2	1.7	1.9	2.1	2.0	1.4	3.4	3.3	2.4	1.1	2.4	1.5	1.6	1.4	1.5
OM5148 #3	1.7	1.9	2.0	1.9	1.5	3.4	2.5	1.7	1.0	1.6	2.0	2.0	1.7	1.9
OM5148 #5	1.9	2.6	2.6	2.7	2.0	4.9	4.3	3.4	1.2	3.2	1.9	2.1	1.6	1.8
OM5148 #6	1.8	3.2	2.6	2.6	2.4	4.7	4.2	3.5	1.1	2.9	2.0	2.3	1.6	1.8
OM5334 #1	1.6	1.9	1.6	2.2	2.7	6.1	10.5	3.6	1.2	6.7	1.6	1.9	1.6	1.8
OM5334 #6	1.7	2.0	1.6	2.0	2.9	5.1	6.1	3.5	1.4	4.7	1.7	1.9	1.5	1.8
OM5334 #7	1.8	2.1	1.8	2.4	3.4	9.2	14.3	5.7	1.1	10.2	2.2	2.2	1.8	2.0
OM5334 #10	1.6	1.9	1.6	2.0	2.1	3.4	5.4	3.1	0.9	5.7	1.7	1.8	1.5	1.8
OM5334 #11	1.7	2.2	1.7	2.5	3.3	8.0	14.4	6.0	1.2	9.6	1.9	2.2	1.6	1.8
OM5001 #3	2.1	2.9	2.8	3.0	2.0	2.3	3.1	2.2	0.9	2.8	3.3	3.4	2.3	2.9
OM5001 #7	2.1	3.5	2.8	3.3	4.5	1.4	5.5	2.3	1.2	3.4	2.3	3.1	1.8	2.4
OM5001 #9	1.9	2.8	2.4	2.7	2.6	1.5	3.5	1.9	1.0	2.9	2.2	2.8	1.7	2.2
OM5001 #10	2.3	4.0	3.2	3.5	2.3	1.3	3.6	2.7	1.1	3.3	3.5	3.5	2.2	3.1
OM5001 #11	2.1	3.4	2.7	2.8	2.2	1.0	2.9	2.3	1.0	2.2	3.8	4.0	2.3	2.8
OM5365 #1	1.5	1.9	2.0	1.8	2.4	5.9	4.4	4.5	1.5	9.4	1.6	2.1	1.5	1.2
OM5365 #2	1.6	2.2	2.1	2.1	3.1	3.9	3.8	3.0	1.2	6.2	2.3	3.8	1.6	1.7
OM5365 #4	1.9	2.4	2.6	2.3	2.5	4.5	3.1	2.2	1.1	2.8	ND	ND	1.5	2.2
CIRC 0196 #2	1.9	2.6	2.8	2.6	2.2	1.7	1.3	2.1	0.8	5.1	4.4	7.6	2.4	3.6
CIRC 0196 #3	1.7	2.2	2.2	2.2	2.1	1.7	1.3	1.5	0.7	1.3	4.4	24.0	2.8	3.7
CIRC 0196 #4	1.9	2.6	2.7	2.6	1.6	1.7	1.3	1.9	0.9	4.2	5.2	7.5	2.8	4.6
CIRC 0196 #5	1.6	2.1	2.0	2.1	1.7	1.7	1.3	1.5	0.7	1.4	3.8	5.6	2.8	3.6
CIRC 0196 #6	2.0	3.3	2.7	2.5	1.7	1.7	1.4	2.0	0.8	3.6	4.3	5.1	2.5	6.8
OM5346 #2	1.7	2.9	2.4	3.6	4.3	1.5	1.5	9.9	0.9	6.0	2.2	8.5	1.8	2.2
OM5346 #3	1.9	2.3	1.4	1.5	5.2	4.3	3.7	1.7	0.7	1.3	2.4	22.3	2.0	2.2
OM5346 #4	2.1	4.7	3.5	5.8	4.9	1.4	1.9	16.5	1.0	12.6	2.2	7.2	1.9	ND
OM5346 #5	1.9	3.2	3.4	3.2	5.2	1.4	6.4	1.6	0.9	1.3	2.0	3.8	1.6	1.7
OM5162 #1	2.7	8.7	7.2	6.3	5.6	1.5	16.8	4.8	1.3	1.8	2.1	2.1	1.7	0.9
OM5162 #3	1.5	1.8	1.8	1.8	0.5	2.0	1.2	1.9	1.2	1.6	1.9	2.1	1.6	1.1
OM5162 #11	1.5	2.2	2.1	2.1	0.5	2.9	1.3	2.7	1.6	1.8	2.1	2.4	1.5	1.1
OM5162 #13	1.7	2.5	2.3	2.3	0.6	2.3	1.3	2.3	1.7	2.3	2.2	3.3	1.6	1.3
OM5162 #15	0.7	2.1	2.3	2.0	0.6	2.2	1.2	2.5	1.7	1.8	2.0	2.6	1.5	1.1
OM5267 #1	2.1	3.0	4.0	3.3	2.7	3.9	6.7	1.6	0.4	1.8	2.4	4.3	1.7	1.8
OM5267 #4	1.7	1.8	2.0	2.2	2.6	2.9	3.4	1.7	0.5	1.7	2.3	11.2	2.1	1.8
OM5267 #5	1.9	3.0	3.7	3.5	3.2	4.4	5.2	1.5	0.4	1.7	2.3	13.1	2.1	1.8
OM5267 #8	1.6	1.9	2.0	2.1	5.8	1.5	5.5	1.6	0.7	2.0	2.1	5.1	1.9	1.5

>7
5-7
4-5
3-4
2-3
0-2

C **Each antibody used at neutralization IC_{80} concentration**

	CD4 Binding Site				V3 Glycan			V1/V2			MPER (gp41)			
	VRC01	VRC07-523	3BNC117	N6	PGT121	2G12	10-1074	PGDM1400	CAP256.VRC26.25	PG9	10E8	10E8v4-V5R-100cF	2F5	4E10
OM5148 #1	1.5	0.9	1.8	1.1	2.9	3.5	6.7	2.2	1.5	3.4	1.6	1.7	1.4	1.1
OM5148 #2	1.9	2.1	2.4	2.3	1.6	3.5	2.6	2.6	1.3	3.0	1.4	1.6	1.4	1.5
OM5148 #3	2.0	2.2	2.2	2.3	1.5	3.2	2.3	1.9	0.8	1.9	1.7	1.8	1.6	1.6
OM5148 #5	2.0	2.2	2.4	2.3	1.7	3.6	2.6	2.6	1.0	3.4	1.8	1.9	1.7	1.6
OM5148 #6	1.8	2.1	2.2	2.2	1.6	3.4	2.0	2.6	1.1	2.1	1.8	2.1	1.8	1.6
OM5334 #1	2.5	2.8	2.1	3.1	5.7	9.7	7.9	6.2	2.4	14.7	1.6	1.7	1.6	1.6
OM5334 #6	2.4	2.7	2.0	3.0	4.1	8.3	8.1	6.1	2.2	21.6	1.6	1.8	1.7	1.7
OM5334 #7	2.9	3.5	2.4	4.7	8.7	13.9	9.1	10.4	3.2	26.7	1.9	2.1	2.0	1.7
OM5334 #10	2.1	2.6	2.0	3.1	3.9	7.6	5.0	5.8	1.6	15.4	1.6	1.7	1.5	1.6
OM5334 #11	2.2	2.8	2.1	3.2	8.1	11.1	10.6	8.5	3.5	20.1	1.8	1.9	1.6	1.6
OM5001 #3	2.4	3.1	2.6	2.9	1.6	2.8	1.8	2.2	0.7	3.4	2.5	2.6	2.0	2.0
OM5001 #7	2.4	4.6	3.2	3.7	2.9	1.6	2.4	2.5	0.5	4.8	2.0	2.4	1.8	1.9
OM5001 #9	2.4	3.7	2.9	3.6	2.0	2.2	2.8	2.7	0.5	8.6	1.9	2.3	1.8	1.8
OM5001 #10	2.7	3.7	4.1	4.0	3.5	2.5	3.1	3.0	1.5	2.4	2.9	3.1	2.2	2.4
OM5001 #11	3.2	6.5	4.5	4.8	2.3	1.5	2.1	3.6	0.6	5.3	3.0	3.8	2.5	2.1
OM5365 #1	2.1	2.4	2.5	2.2	1.9	7.5	1.9	7.4	1.3	18.7	1.5	1.8	1.5	1.2
OM5365 #2	1.5	1.8	1.8	1.8	2.2	3.0	1.4	2.3	1.2	6.4	3.4	4.2	2.4	1.5
OM5365 #4	1.9	2.4	2.5	2.2	3.3	5.7	3.4	2.5	1.6	7.8	3.2	6.8	3.0	2.9
CIRC 0196 #2	2.6	4.8	4.3	4.0	1.2	1.9	0.8	3.1	0.6	10.3	3.2	4.7	2.7	2.4
CIRC 0196 #3	2.3	2.5	3.8	3.7	0.7	1.9	0.6	1.8	0.4	1.2	4.0	9.6	3.2	2.4
CIRC 0196 #4	3.2	5.0	5.0	5.8	0.9	2.1	0.7	3.9	0.6	11.1	2.9	3.4	2.4	2.1
CIRC 0196 #5	5.2	4.1	2.9	4.3	1.8	2.3	0.8	2.3	0.7	1.7	3.0	3.2	2.4	2.3
CIRC 0196 #6	9.9	3.3	6.8	7.0	1.4	2.7	0.8	3.6	0.5	9.6	2.5	2.8	2.2	1.8
OM5346 #2	1.6	2.6	1.9	3.1	1.4	1.2	1.1	4.0	2.3	6.8	2.1	3.1	2.1	2.0
OM5346 #3	1.9	2.1	1.4	1.4	1.8	3.5	1.7	1.6	0.5	1.1	2.6	3.9	2.5	1.9
OM5346 #4	1.8	3.0	2.3	3.4	1.3	1.3	1.0	5.9	4.7	8.3	2.9	6.0	1.1	2.1
OM5346 #5	1.7	2.5	2.4	2.4	2.8	1.3	2.8	1.2	1.5	1.0	2.3	2.5	1.8	1.8
OM5162 #1	3.9	12.4	10.6	8.6	7.8	1.6	8.7	6.5	0.5	2.4	2.1	2.1	1.6	1.0
OM5162 #3	1.7	2.3	2.1	2.2	0.7	2.4	0.8	2.4	2.2	1.9	1.8	1.8	1.6	1.1
OM5162 #11	2.0	2.8	2.4	2.3	0.8	3.2	0.8	3.1	3.9	2.1	2.4	2.4	2.0	1.1
OM5162 #13	1.5	1.8	1.8	1.8	0.9	2.0	0.9	1.9	3.9	1.9	2.2	2.2	1.7	1.2
OM5162 #15	1.4	1.6	1.7	1.6	0.6	2.1	0.9	1.9	2.7	2.4	2.1	2.1	1.8	1.1
OM5267 #1	2.6	3.6	4.3	3.7	1.2	3.4	1.7	1.4	0.4	2.0	2.3	4.3	2.1	1.7
OM5267 #4	1.6	2.0	2.0	2.4	1.4	3.3	1.0	1.5	0.4	1.4	2.3	4.4	2.4	1.6
OM5267 #5	2.4	4.7	4.9	4.3	1.5	5.3	1.6	1.5	0.5	1.5	2.5	5.0	2.4	1.6
OM5267 #8	1.8	3.2	2.4	2.6	2.2	1.7	1.7	1.5	0.6	2.0	2.3	2.8	1.9	1.5

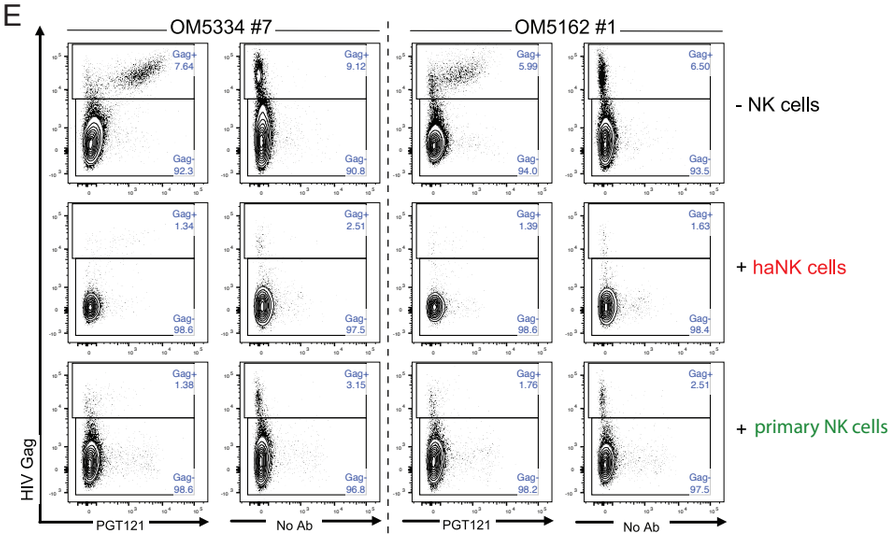

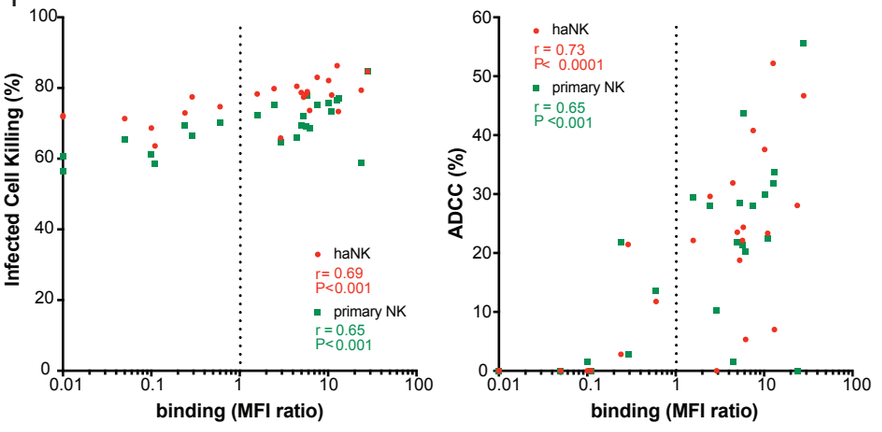

D **Binding coverage of antibody combinations (@IC_{80} concentration)**

		CD4 binding sites				V3-Glycan			V1/V2			MPER			
		VRC01	VRC07-523	3BNC117	N6	PGT121	2G12	10-1074	PGDM1400	CAP256. VRC26.25	PG9	10E8	10E8v4-V5R-100cF	2F5	4E10
CD4 binding site	VRC01	61%													
	VRC07-523	89%	89%												
	3BNC117	83%	89%	83%											
	N6	86%	89%	86%	86%										
V3-Glycar	PGT121	75%	94%	89%	92%	42%									
	2G12	89%	100%	97%	100%	89%	75%								
	10-1074	75%	92%	86%	89%	53%	86%	47%							
V1/V2	PGDM1400	83%	94%	92%	92%	78%	92%	78%	72%						
	CAP256. VRC26.25	75%	94%	92%	92%	58%	81%	64%	78%	28%					
	PG9	86%	97%	94%	94%	78%	94%	81%	81%	81%	75%				
MPER	10E8	89%	97%	97%	97%	83%	100%	94%	97%	78%	94%	64%			
	10E8v4-V5R-100cF	92%	97%	97%	97%	86%	100%	94%	97%	86%	94%	72%	72%		
	2F5	75%	92%	92%	92%	75%	86%	83%	86%	67%	89%	64%	72%	47%	
	4E10	69%	89%	86%	86%	61%	86%	67%	75%	50%	81%	64%	72%	50%	28%

Fig. 4

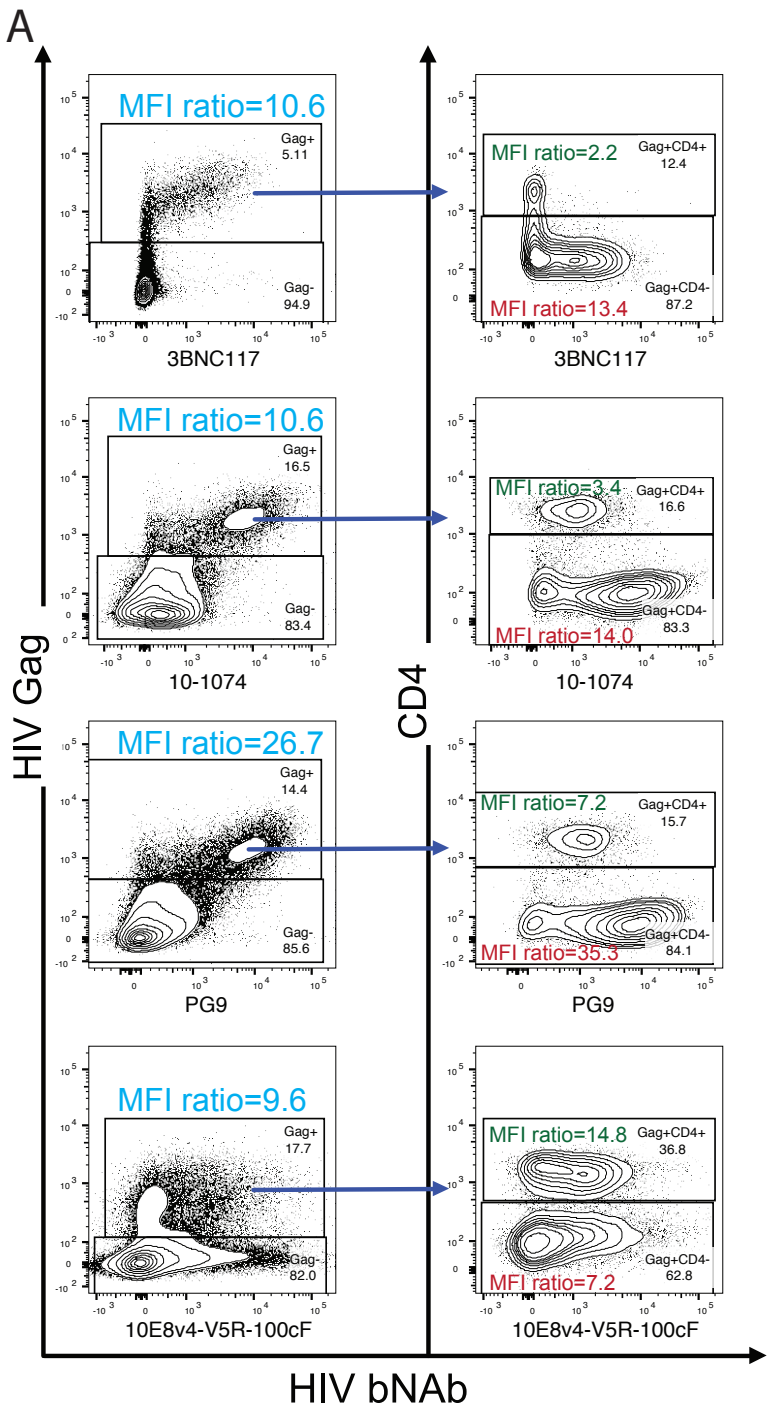
A
MFI ratio=10.6
Gag+ 5.11
Gag- 94.9
3BNC117
MFI ratio=2.2
Gag+CD4+ 12.4
MFI ratio=13.4
Gag+CD4- 87.2
3BNC117
MFI ratio=10.6
Gag+ 16.5
Gag- 83.4
10-1074
MFI ratio=3.4
Gag+CD4+ 16.6
Gag+CD4- 83.3
MFI ratio=14.0
10-1074
MFI ratio=26.7
Gag+ 14.4
Gag- 85.6
PG9
MFI ratio=7.2
Gag+CD4+ 15.7
Gag+CD4- 84.1
MFI ratio=35.3
PG9
MFI ratio=9.6
Gag+ 17.7
Gag- 82.0
10E8v4-V5R-100cF
MFI ratio=14.8
Gag+CD4+ 36.8
Gag+CD4- 62.8
MFI ratio=7.2
10E8v4-V5R-100cF
HIV Gag
CD4
HIV bNAb

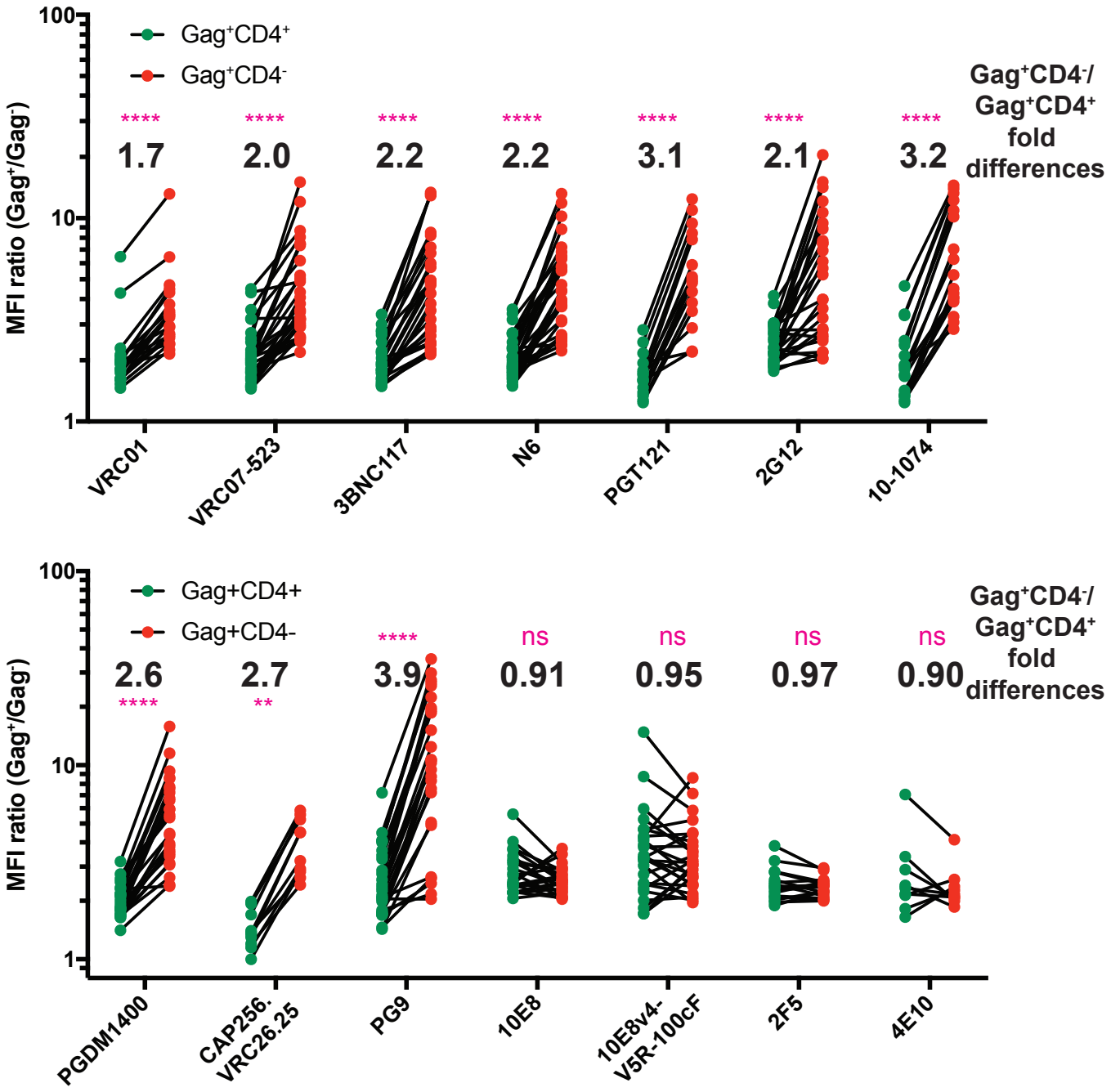
B
MFI ratio (Gag+/Gag-)
Gag+CD4+
Gag+CD4-
****
1.7
2.0
2.2
2.2
3.1
2.1
3.2
Gag+CD4-/ Gag+CD4+ fold differences
VRC01
VRC07-523
3BNC117
N6
PGT121
2G12
10-1074
Gag+CD4+
Gag+CD4-
2.6
2.7
3.9
0.91
0.95
0.97
0.90
****
**
ns
Gag+CD4-/ Gag+CD4+ fold differences
PGDM1400
CAP256. VRC26.25
PG9
10E8
10E8v4- V5R-100cF
2F5
4E10

Fig. 5

A

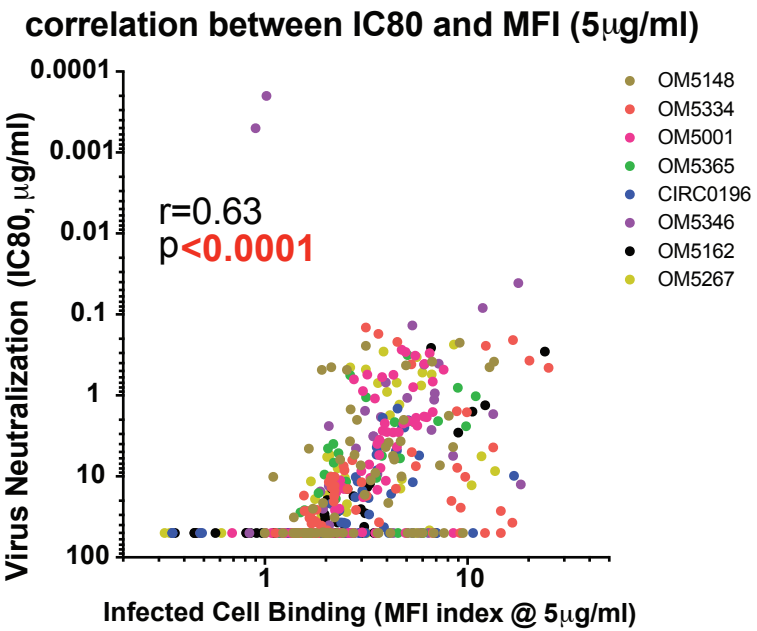
correlation between IC80 and MFI (5μg/ml)
Virus Neutralization (IC80, μg/ml)
Infected Cell Binding (MFI index @ 5μg/ml)
r=0.63
p<0.0001
OM5148
OM5334
OM5001
OM5365
CIRC0196
OM5346
OM5162
OM5267

B

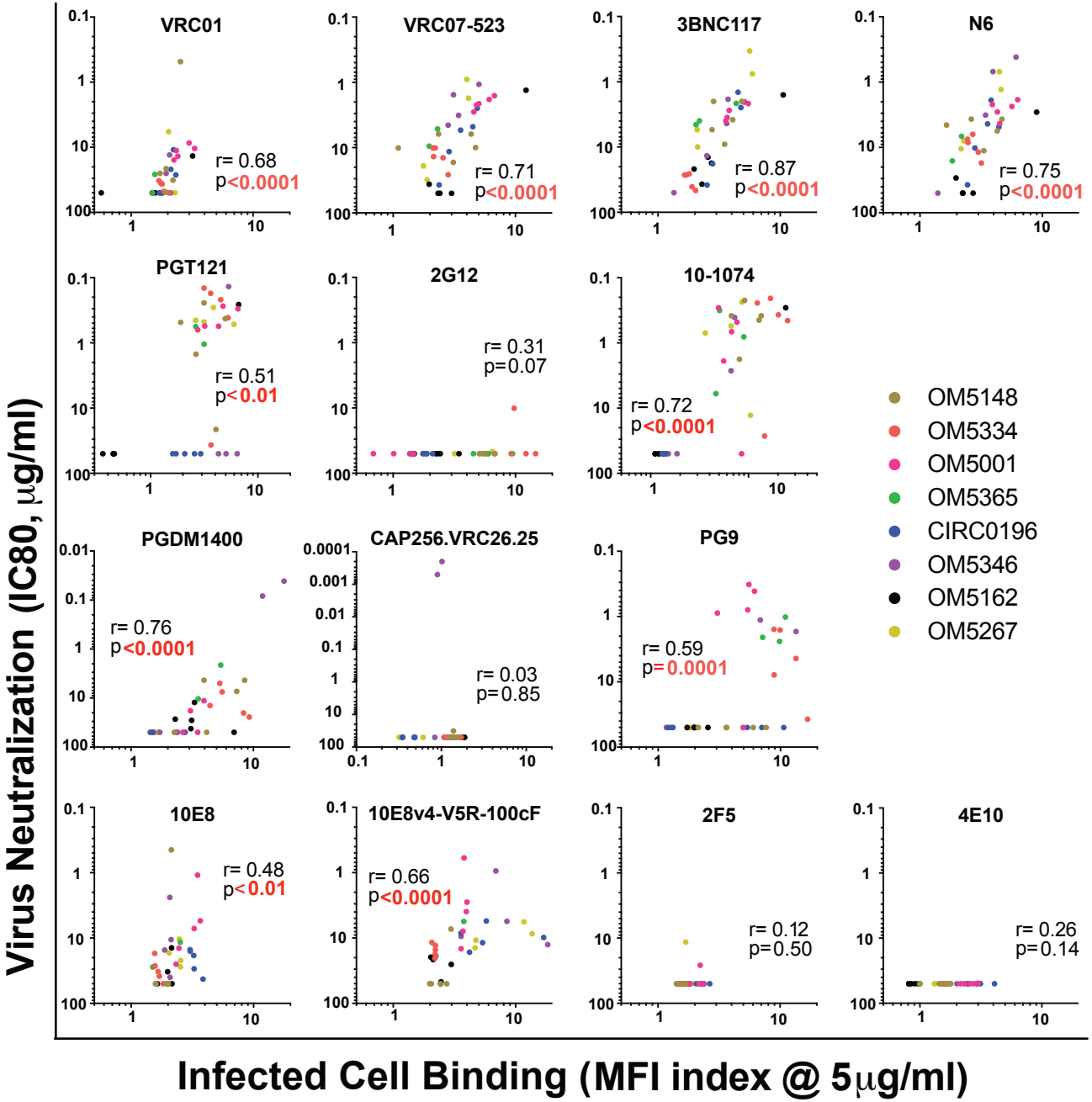
VRC01
r= 0.68
p<0.0001
VRC07-523
r= 0.71
p<0.0001
3BNC117
r= 0.87
p<0.0001
N6
r= 0.75
p<0.0001
PGT121
r= 0.51
p<0.01
2G12
r= 0.31
p=0.07
10-1074
r= 0.72
p<0.0001
PGDM1400
r= 0.76
p<0.0001
CAP256.VRC26.25
r= 0.03
p=0.85
PG9
r= 0.59
p=0.0001
10E8
r= 0.48
p<0.01
10E8v4-V5R-100cF
r= 0.66
p<0.0001
2F5
r= 0.12
p=0.50
4E10
r= 0.26
p=0.14
OM5148
OM5334
OM5001
OM5365
CIRC0196
OM5346
OM5162
OM5267
Virus Neutralization (IC80, μg/ml)
Infected Cell Binding (MFI index @ 5μg/ml)

sFig. 1

	CD4 binding sites				V3-glycan			V1/V2			MPER (gp41)			
	VRC01	VRC07 -523	3BNC117	N6	PGT121	2G12	10-1074	PGDM1400	CAP256. VRC26.25	PG9	10E8	10E8v4-V5R-100cF	2F5	4E10
OM5148 #1	1.9	1.0	2.7	1.5	8.4	5.7	14.5	3.8	3.6	8.3	1.7	1.9	1.5	1.0
OM5148 #2	2.3	2.6	3.5	3.1	2.1	6.1	3.9	4.5	1.7	4.9	1.6	2.1	1.6	1.7
OM5148 #3	2.9	4.1	4.3	4.4	3.4	6.9	5.3	2.6	1.1	3.0	1.7	2.1	1.8	1.7
OM5148 #5	3.1	3.8	4.9	4.4	3.6	7.8	7.0	6.7	1.9	10.3	1.8	2.3	1.9	1.7
OM5148 #6	2.5	3.5	3.8	4.0	3.4	9.5	4.5	6.6	2.0	5.1	2.0	2.6	2.0	1.8
OM5334 #1	2.7	3.0	2.2	3.7	7.9	14.2	10.9	8.6	2.9	19.2	1.5	2.0	1.7	1.7
OM5334 #6	2.6	2.9	2.1	3.7	5.9	12.1	12.2	8.5	2.8	29.9	1.5	2.0	1.8	1.8
OM5334 #7	3.4	4.3	2.9	6.3	12.4	20.5	13.3	15.8	4.5	35.3	1.8	2.1	2.0	1.8
OM5334 #10	2.3	3.0	2.1	3.7	5.0	10.7	6.3	7.7	2.1	19.7	1.6	2.0	1.6	1.8
OM5334 #11	2.4	3.2	2.3	3.9	10.9	15.1	14.0	11.5	4.5	25.7	1.7	2.1	1.6	1.7
OM5001 #3	3.8	7.5	5.7	6.5	2.9	2.8	2.7	3.6	0.5	10.7	2.7	3.2	2.3	2.3
OM5001 #7	2.9	7.3	4.7	5.5	4.8	1.6	3.3	3.1	0.4	8.7	2.1	2.9	1.9	2.0
OM5001 #9	3.3	7.5	4.9	6.8	3.8	2.2	4.0	3.4	0.4	15.1	2.2	3.1	1.9	2.0
OM5001 #10	3.3	5.2	6.0	5.8	5.1	2.9	4.1	3.5	1.7	2.7	3.0	3.4	2.2	2.6
OM5001 #11	4.3	12.0	8.2	8.8	3.5	1.4	3.1	5.9	0.6	10.6	2.9	3.8	2.6	2.1
OM5365 #1	2.1	2.6	2.6	2.2	2.0	8.9	2.0	9.3	1.3	22.4	1.5	1.9	1.5	1.2
OM5365 #2	1.4	1.9	1.8	1.8	2.2	3.2	1.4	2.4	1.3	7.6	3.5	4.0	2.5	1.4
OM5365 #4	2.0	2.9	3.2	2.6	4.4	7.5	4.3	3.1	1.9	12.5	3.7	8.6	3.0	4.1
CIRC 0196 #2	3.5	4.9	8.5	7.2	1.2	1.9	0.7	5.9	0.3	26.6	2.6	3.6	2.5	2.1
CIRC 0196 #3	2.4	3.5	4.8	4.7	0.5	1.8	0.5	1.7	0.2	1.1	3.1	7.1	2.9	2.0
CIRC 0196 #4	4.7	8.7	13.1	13.2	0.7	2.0	0.7	5.5	0.3	27.5	2.5	2.6	2.2	1.9
CIRC 0196 #5	6.4	3.2	4.9	6.5	2.6	2.5	0.9	2.4	0.3	2.0	2.8	3.2	2.4	2.2
CIRC 0196 #6	13.2	8.1	12.9	11.9	1.4	2.6	0.8	5.4	0.3	18.6	2.1	2.4	2.1	1.7
OM5346 #2	1.6	2.6	1.9	3.2	1.4	1.1	1.1	4.4	2.4	7.2	2.1	3.1	2.1	2.0
OM5346 #3	2.0	2.2	1.3	1.3	1.7	4.0	1.7	1.5	0.3	0.9	2.4	3.5	2.4	1.9
OM5346 #4	1.8	3.1	2.4	3.7	1.3	1.3	0.9	7.2	5.2	9.5	2.9	5.8	0.9	2.4
OM5346 #5	1.7	2.6	2.5	2.5	2.9	1.3	2.9	1.2	1.5	1.0	2.2	2.4	1.7	1.7
OM5162 #1	4.5	15.0	13.4	10.2	9.4	1.6	10.2	7.6	0.5	2.5	2.1	2.0	1.5	0.9
OM5162 #3	1.8	2.5	2.2	2.4	0.6	2.7	0.8	2.6	2.6	1.9	1.7	1.7	1.5	1.0
OM5162 #11	2.0	3.2	2.8	2.6	0.7	4.0	0.7	3.9	5.6	2.2	2.5	2.4	2.0	1.1
OM5162 #13	1.6	2.1	2.0	2.0	0.7	2.0	0.8	2.2	5.8	2.1	2.2	2.2	1.6	1.1
OM5162 #15	1.4	1.7	1.8	1.6	0.5	2.2	0.8	2.1	3.2	2.6	2.0	2.0	1.8	1.1
OM5267 #1	2.9	5.0	6.7	5.6	1.3	5.3	2.2	1.4	0.4	2.4	2.4	4.4	2.0	1.6
OM5267 #4	1.6	2.0	2.0	2.4	1.4	3.6	1.0	1.5	0.4	1.4	2.3	4.5	2.4	1.6
OM5267 #5	2.7	6.2	7.2	5.8	1.7	7.5	1.9	1.4	0.4	1.6	2.6	5.2	2.4	1.5
OM5267 #8	1.8	3.2	2.4	2.7	2.2	1.6	1.7	1.4	0.6	2.0	2.3	2.7	1.9	1.5

>10
7-10
5-7
4-5
3-4
2-3
0-2

sFig. 2

A

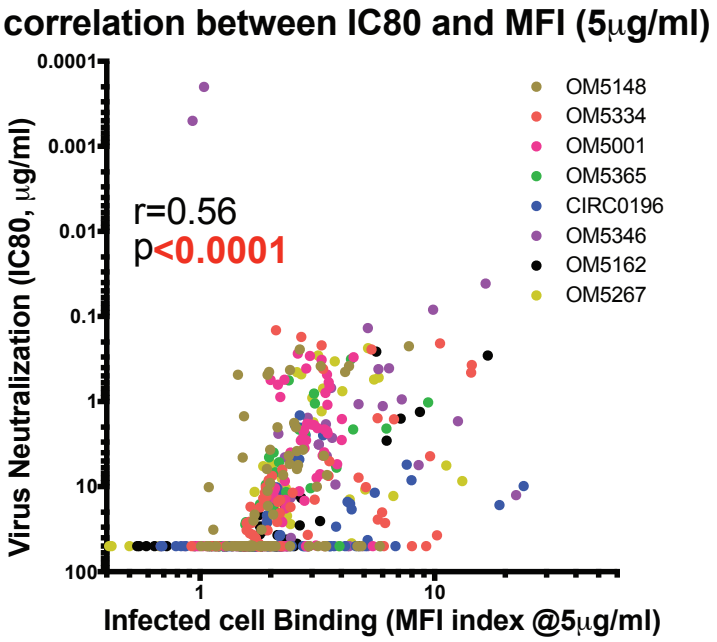
correlation between IC80 and MFI (5μg/ml)
r=0.56
p<0.0001
Virus Neutralization (IC80, μg/ml)
Infected cell Binding (MFI index @5μg/ml)
OM5148
OM5334
OM5001
OM5365
CIRC0196
OM5346
OM5162
OM5267

B

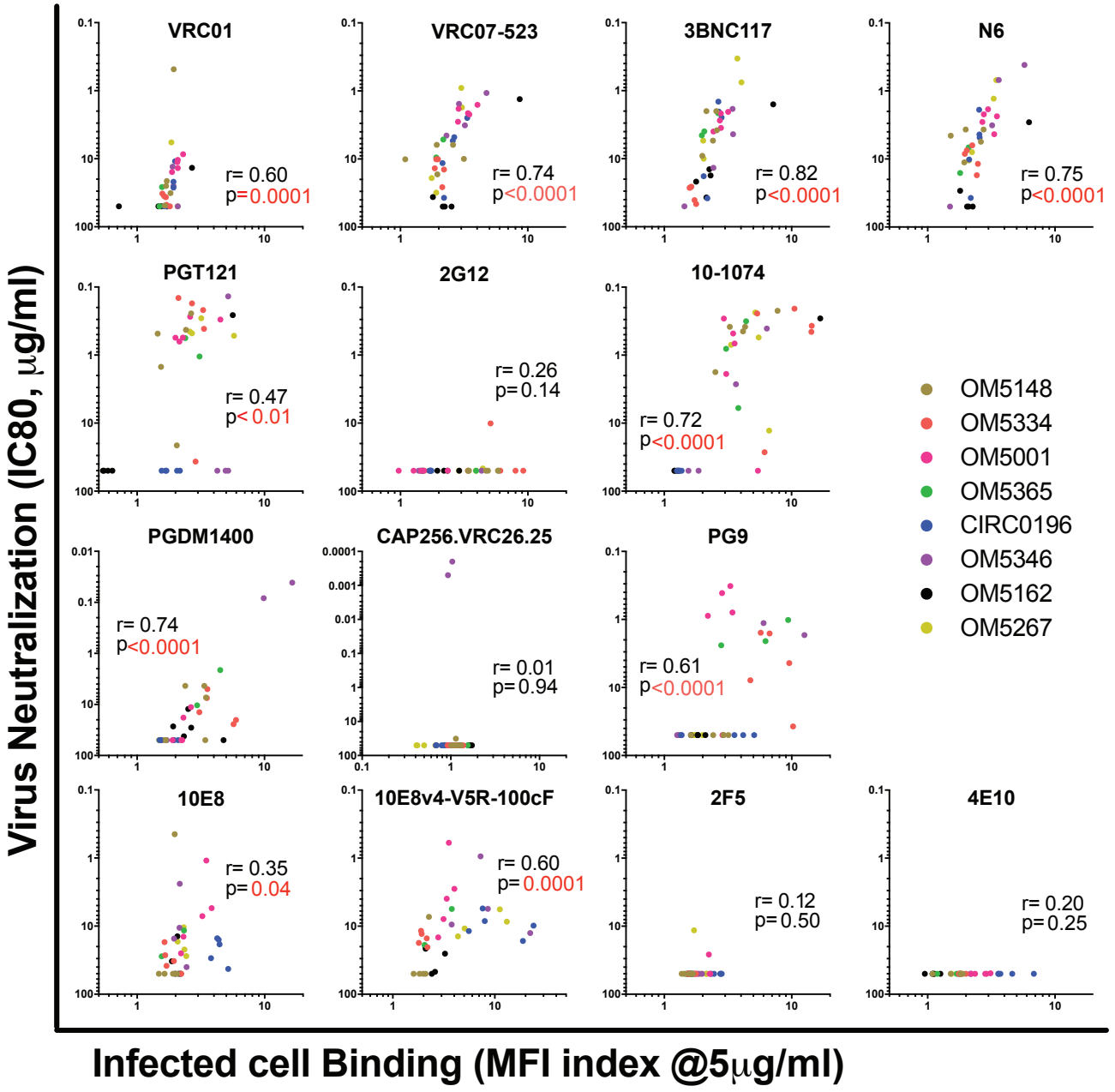
VRC01
r= 0.60
p=0.0001
VRC07-523
r= 0.74
p<0.0001
3BNC117
r= 0.82
p<0.0001
N6
r= 0.75
p<0.0001
PGT121
r= 0.47
p< 0.01
2G12
r= 0.26
p=0.14
10-1074
r= 0.72
p<0.0001
PGDM1400
r= 0.74
p<0.0001
CAP256.VRC26.25
r= 0.01
p=0.94
PG9
r= 0.61
p<0.0001
10E8
r= 0.35
p=0.04
10E8v4-V5R-100cF
r= 0.60
p=0.0001
2F5
r= 0.12
p=0.50
4E10
r= 0.20
p=0.25
OM5148
OM5334
OM5001
OM5365
CIRC0196
OM5346
OM5162
OM5267
Virus Neutralization (IC80, μg/ml)
Infected cell Binding (MFI index @5μg/ml)

sFig. 3

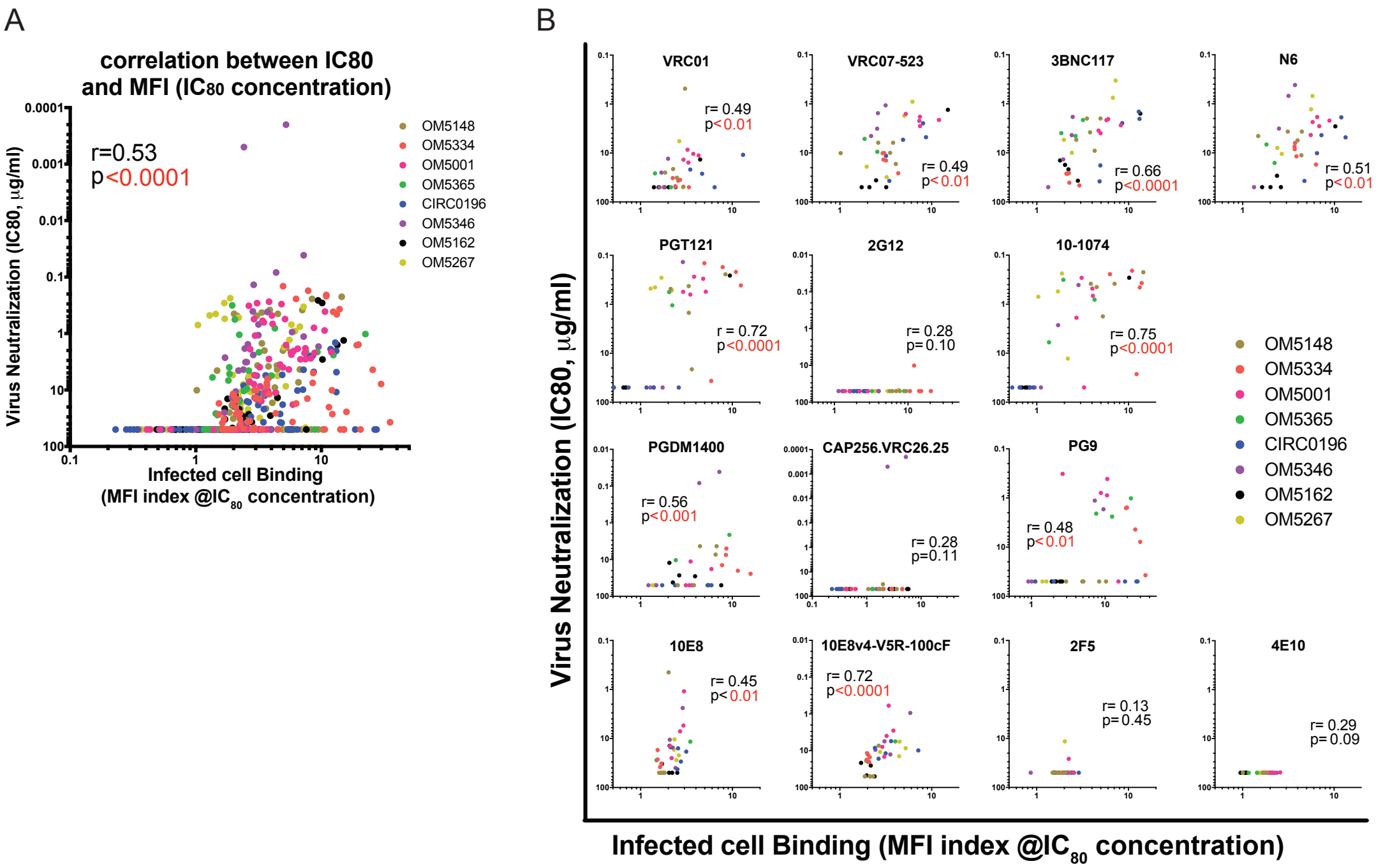
A
correlation between IC80
and MFI (IC80 concentration)
r=0.53
p<0.0001
Virus Neutralization (IC80, μg/ml)
Infected cell Binding
(MFI index @IC80 concentration)
OM5148
OM5334
OM5001
OM5365
CIRC0196
OM5346
OM5162
OM5267
B
VRC01
r= 0.49
p<0.01
VRC07-523
r= 0.49
p<0.01
3BNC117
r= 0.66
p<0.0001
N6
r= 0.51
p<0.01
PGT121
r = 0.72
p<0.0001
2G12
r= 0.28
p= 0.10
10-1074
r= 0.75
p<0.0001
PGDM1400
r= 0.56
p<0.001
CAP256.VRC26.25
r= 0.28
p=0.11
PG9
r= 0.48
p< 0.01
10E8
r= 0.45
p< 0.01
10E8v4-V5R-100cF
r= 0.72
p<0.0001
2F5
r= 0.13
p= 0.45
4E10
r= 0.29
p= 0.09
Virus Neutralization (IC80, μg/ml)
Infected cell Binding (MFI index @IC80 concentration)

sFig. 4

A

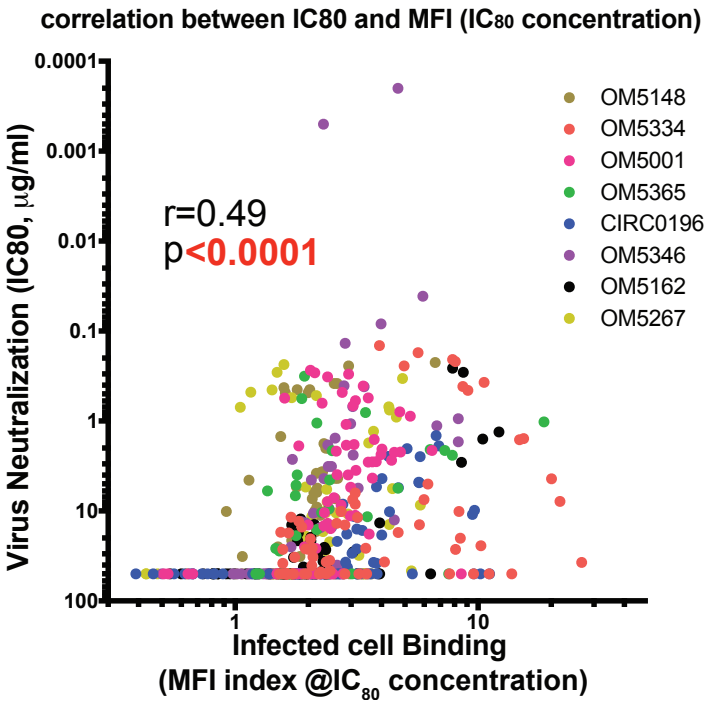
correlation between IC80 and MFI (IC80 concentration)
Virus Neutralization (IC80, μg/ml)
Infected cell Binding
(MFI index @IC80 concentration)
r=0.49
p<0.0001
OM5148
OM5334
OM5001
OM5365
CIRC0196
OM5346
OM5162
OM5267

B

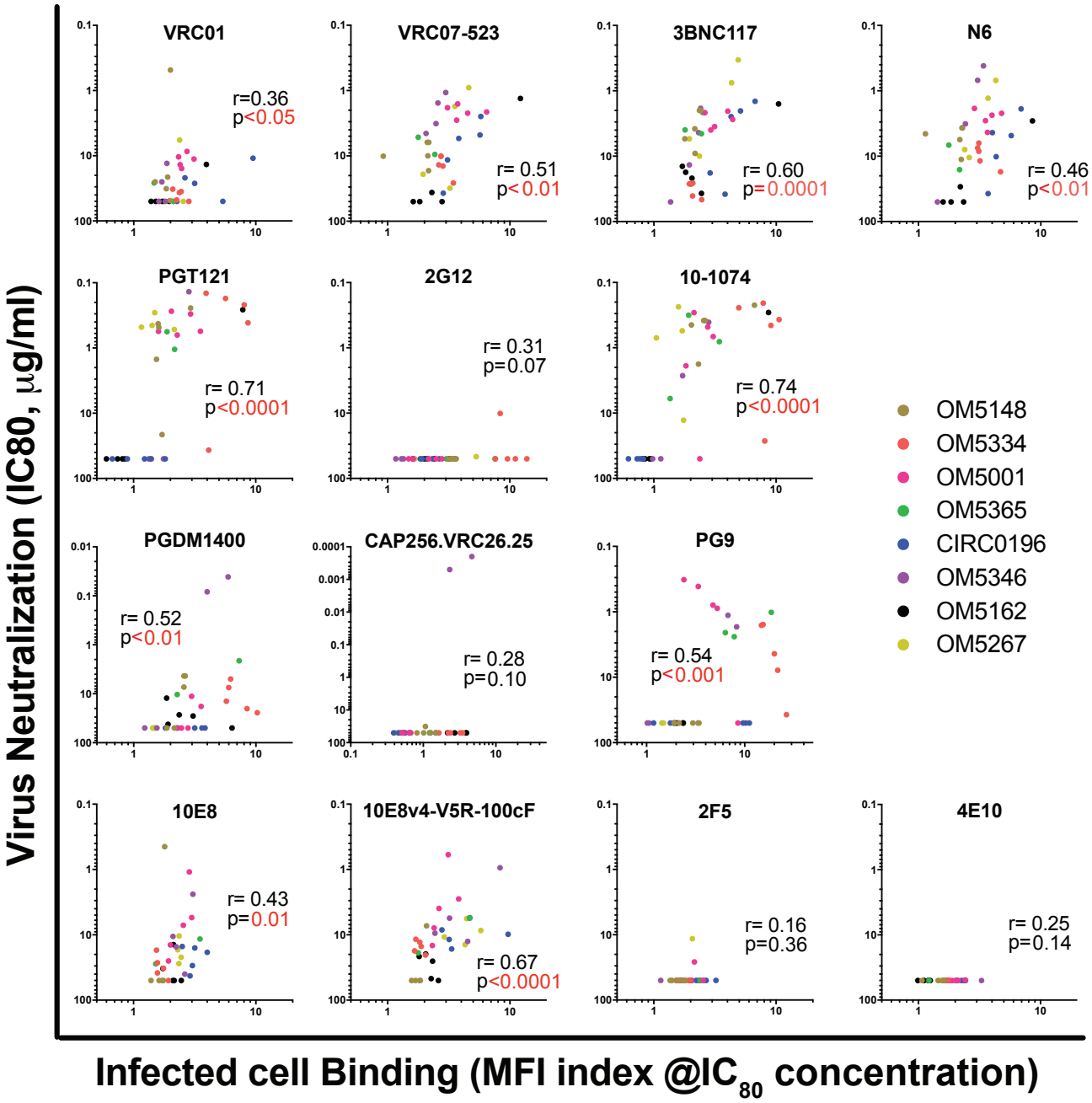
VRC01
r=0.36
p<0.05
VRC07-523
r= 0.51
p< 0.01
3BNC117
r= 0.60
p=0.0001
N6
r= 0.46
p<0.01
PGT121
r= 0.71
p<0.0001
2G12
r= 0.31
p=0.07
10-1074
r= 0.74
p<0.0001
PGDM1400
r= 0.52
p<0.01
CAP256.VRC26.25
r= 0.28
p=0.10
PG9
r= 0.54
p<0.001
10E8
r= 0.43
p=0.01
10E8v4-V5R-100cF
r= 0.67
p<0.0001
2F5
r= 0.16
p=0.36
4E10
r= 0.25
p=0.14
OM5148
OM5334
OM5001
OM5365
CIRC0196
OM5346
OM5162
OM5267
Virus Neutralization (IC80, μg/ml)
Infected cell Binding (MFI index @IC80 concentration)